MASTERARBEIT | MASTER'S THESIS

Titel | Title

Investigation of a marine dinoflagellate and its photosymbiosis with flatworms

verfasst von | submitted by

Marlis Stenzl BSc

angestrebter akademischer Grad | in partial fulfilment of the requirements for the degree of

Master of Science (MSc)

Wien | Vienna, 2024

Studienkennzahl lt. Studienblatt | Degree programme code as it appears on the student record sheet:	UA 066 830
Studienrichtung lt. Studienblatt | Degree programme as it appears on the student record sheet:	Masterstudium Molecular Microbiology, Microbial Ecology and Immunobiology
Betreut von | Supervisor:	Elizabeth Hambleton BA PhD

Abstract

Marine dinoflagellates provide crucial ecological services by forming part of the foundation of the marine food web and participating in photosymbiosis, which sustains coral reefs, the most biodiverse marine ecosystems. However, they can also cause harmful algal blooms (HABs), significantly threatening aquatic life and human health. The dinoflagellate genus *Amphidinium* produces polyketides, toxic secondary metabolites that can accumulate during blooms, leading to fish kills and other environmental hazards. This thesis investigated the growth dynamics of *Amphidinium gibbosum* strain Amp02, indicating that its optimal irradiance level ranges between photon flux densities of 12 to 230 μmol m^{-2} s^{-1}. Understanding these dynamics can inform strategies for controlling blooms, such as limiting light availability.

In addition to their role in HABs, *Amphidinium* dinoflagellates are endosymbionts of various marine heterotrophs, including the acoel flatworm *Waminoa.* To explore whether the symbiosis establishment between *Amphidinium* and *Waminoa* can be controlled, I exposed aposymbiotic *Waminoa* to either cultured algae or symbiotic “donor” flatworms. Cultured algae alone resulted in transient infections, whereas exposure to symbiotic donors consistently led to stable associations.

An understudied aspect of marine photosymbiosis is the potential defensive role of dinoflagellates mediated by polyketide production. In this context, Sandra Montaño Salazar and I aimed to develop a method using HRES-HPLC-MS/MS to identify polyketides in *Amphidinium* cultures and symbiotic *Waminoa* flatworms. While definite identification of polyketides was not yet achieved, we established a preliminary workflow for metabolite identification, laying the groundwork for future studies.

Zusammenfassung

Marine Dinoflagellaten leisten entscheidende ökologische Dienste, indem sie Teil des Fundamentes des marinen Nahrungsnetzes bilden und in Photosymbiosen teilnehmen, welche Korallenriffe – die biodiversesten marinen Ökosysteme – erhalten. Sie können jedoch auch schädliche Algenblüten (HABs) verursachen, welche eine erhebliche Bedrohung für aquatisches Leben und menschliche Gesundheit darstellen. Die Dinoflagellaten-Gattung *Amphidinium* produziert Polyketide, toxische Sekundärmetaboliten, deren Akkumulation während Algenblüten zu Fischsterben sowie anderen Umweltrisiken führen kann. Diese These hat die Wachstumsdynamik des *Amphidinium gibbosum* Stammes Amp02 untersucht und gezeigt, dass dessen optimales Lichtniveau zwischen Photonenflussdichten von 12 bis 230 μmol m^{-2} s^{-1} liegt. Ein Verständnis dieser Dynamiken kann die Entwicklung von Kontrollstrategien für Algenblüten unterstützen, beispielsweise durch die Einschränkung der Lichtverfügbarkeit.

Zusätzlich zu ihrer Rolle in schädlichen Algenblüten sind *Amphidinium* Dinoflagellaten Endosymbionten verschiedener mariner Heterotrophen, einschließlich der Acoela-Plattwurmgattung *Waminoa*. Um herauszufinden, ob die Symbiosebildung zwischen *Waminoa* und *Amphidinium* kontrolliert werden kann, habe ich aposymbiotische *Waminoa* entweder kultivierten Algen oder symbiotischen „Spender“ Plattwürmern ausgesetzt. Kultivierte Algen alleine resultierten in transienten Infektionen, während die Behandlung mit symbiotischen Spendern konsistent zu stabilen Assoziationen geführt hat.

Ein wenig erforschter Aspekt der marinen Photosymbiose ist die potenzielle defensive Rolle der Dinoflagellaten, vermittelt durch Polyketidproduktion. In diesem Zusammenhang, haben Sandra Montaño Salazar und Ich angestrebt, eine HRES-HPLC-MS/MS Methode zu entwickeln, um Polyketide in *Amphidinium* Kulturen und symbiotischen *Waminoa* Plattwürmern zu identifizieren. Obwohl wir Polyketide bisher nicht eindeutig identifizieren konnte, haben wir einen vorläufigen Arbeitsablauf etabliert, der die Grundlage zukünftiger Studien bilden wird.

Acknowledgements

First and foremost, I would like to express my deepest gratitude to my group leader and supervisor, Elizabeth (Liz) Hambleton, for giving me the opportunity to join her research team. Her professional guidance, unwavering support, and encouragement played an instrumental role in the completion of this thesis. Working under her supervision has been a truly enriching experience, and I am deeply thankful for the opportunity to learn and grow within her group.

I am especially grateful for Sandra Montaño Salazar for her mentorship and invaluable insights, both of which have significantly shaped my developments as a scientist. The skills and knowledge shared by Liz Hambleton and Sandra Montaño Salazar will stay with me throughout my career, for which I am sincerely thankful.

I would also like to acknowledge Cátia Pinto, our group's animal care technician, whose assistance was vital to my work. Her support throughout the project – whether by reducing my workload or offering fresh perspectives – is immensely appreciated. I am indebted to her for her dedication and willingness to help.

My sincere thanks go to Valentin Göldner, Prof. Wolfgang Wanek, and Rahul Samrat, whose generosity in allowing Sandra and me access to their facilities and expertise was crucial for this research. Their guidance in establishing an HPLC-MS/MS workflow was invaluable and greatly enhanced my work.

I am also very thankful for the insightful conservations I shared with my fellow graduate students, Simone Müller and Stefan Eckensperger. Their enthusiasm to brainstorm and exchange ideas greatly improved my scientific thinking, and their moral support during challenging moments was a source of strength.

A special thank you goes to my partner and fellow researcher, Manuel Uhlir, who has been an endless source of inspiration. His expertise in mass spectrometry analysis proved indispensable when I faced challenges, and I deeply appreciate his help and encouragement.

Lastly, I want to thank my parents and three siblings for their unwavering belief in me. Their constant moral and financial support throughout my academic journey made this achievement possible, and I am forever thankful.

Table of Contents

1. Introduction

1.1. Photosymbiosis between dinoflagellates and animals

Symbiosis is the long-term association between organisms that are unlike each other, encompassing the full spectrum of trophic interactions.[1] As a global phenomenon, all animals and plants engage in symbioses and harbour hundreds to thousands of distinct microbial species.[2] There are different subtypes of symbiosis. One of them, photosynthetic symbiosis or "photosymbiosis", is characterised by eukaryotic heterotrophs hosting photosynthetic microbes ("photosymbionts").[3] This partnership is primarily based on nutrient exchanges.[4] The photosymbiont recycles the heterotroph's inorganic waste into organic matter and transfers photosynthetically produced compounds back to the host.[5-8]

In the ocean, this photosymbiotic nutrient exchange allows the exploitation of oligotrophic, shallow and topical waters by a diverse range of protist and metazoan hosts harbouring microalgae.[9,10] This effect is prominent in coral reefs, which, despite being located in nutrient-poor waters, are the most biodiverse and productive marine ecosystems, rivalling rain forests in the magnitude of ecological services.[11-13] While coral reefs only cover 0.2% of the ocean surface, they support an estimated quarter of all described marine species.[14] The success of coral reef ecosystems is founded on photosymbioses between marine invertebrates and dinoflagellates.[13,15]

1.2. Free-living dinoflagellates

Dinoflagellates, a type of eukaryotic microalgae, are among the most ubiquitous marine photosymbionts.[9] They associate with various protist and invertebrate hosts, including corals, sponges, giant clams, and acoel flatworms.[16] Besides being photosymbionts, dinoflagellates provide a plethora of other ecological functions. Notably, they form the fundament of aquatic food webs, and some cause harmful algal blooms (HABs).[17,18]

Algae blooms are the rapid growth of aquatic phytoplankton,[19] and their occurrence has increased over the last few decades, causing detrimental environmental effects.[20] Blooms of toxin-producing algae can lead to fish mortalities, and toxins can accumulate in the

food chain, ultimately threatening marine life and human health.[21] A concession of environmental factors causes HABs.[22] Among them is light limitation, which is reported to decrease the growth rate of cyanobacteria, hindering bloom formation.[23]

The HAB-causing dinoflagellate genus *Amphidinium* has harboured special attention due to its propensity to produce polyketides, toxic secondary metabolites.[24] While polyketides from *Amphidinium sp.* have been studied extensively due to their antimicrobial, antitumour and cytotoxic properties,[25] they also cause fish kills during blooms.[26] The effects of light availability on the growth rate of *Amphidinium* dinoflagellates are so far unknown.

Therefore, I followed the growth dynamics of a laboratory strain of *Amphidinium gibbosum* (strain "Amp02") kept at either low or high irradiance levels by measuring the cultures' densities via fluorescence and bright-field automated cell counting. I hypothesise that cultures grown at high irradiance levels have an increased growth rate, as reported for other microalgae in the past.[27] Studying growth dynamics, especially under different light conditions, can improve the effectiveness of shading strategies to control HABs, which are more affordable than nutrient limitation.[22,28]

1.3. Dinoflagellates symbiotic with *Waminoa* flatworms

While *Amphidinium sp.* occurs free-living, it is also an endosymbiont of different marine animals like the reef-dwelling acoel flatworm genus *Waminoa* (which includes both described and undescribed species and is referred to hereafter as "*Waminoa"*).[29] Currently, we are establishing *Waminoa* (Convolutidae, Acoela)[30] as a model system for marine photosymbioses. So far, corals have been extensively used for these purposes.[31] However, very little research has been done to understand marine photosymbiosis between dinoflagellates and animals other than corals and related cnidarians, exemplified by the study efforts of marine photosymbiotic nutrient exchange. The mechanisms of nutrient exchanges between flatworms and their endosymbionts remain elusive, with only one report confirming the transfer of algal sterols to the acoel host.[32] On the other hand, the importance of nutrient exchange in cnidarian-dinoflagellate associations has been studied extensively, making it reasonable to assume similar workings in other marine

invertebrate systems hosting dinoflagellates like *Waminoa*.[32,33]

In addition, compared to corals, *Waminoa* is easier to manage.[34] Due to its small size, thousands of individuals can be maintained in limited space. Simple menthol treatments developed by our animal care technician, Cátia Pinto, allow the generation of aposymbiotic animals, which can survive long-term by being fed with the common aquaculture crustaceans *Artemia* and *Tisbe*. Moreover, *Waminoa* reproduce both asexually and sexually under laboratory conditions, producing viable offspring.

Waminoa exhibits two distinct morphologies: some are heart-shaped (obcordate), while others are molar-shaped, both with a notch at the posterior end.[35,36] Their colouration ranges from translucent white to brown.[37,38] White individuals lack endosymbiotic dinoflagellates, contributing to the brown colouration in symbiotic specimens.[36]

Reportedly, *Waminoa* engages in a tripartite photosymbiosis with *Amphidinium* and *Symbiodiniaceae* dinoflagellates.[37,38] Various studies conclude the smaller *Symbiodiniaceae* (diameter 4-8 μm) to be more prevalent than the bigger *Amphidinium* dinoflagellates (diameter 11-16 μm).[37] Nevertheless, we are not able to identify *Symbiodiniaceae* in our *Waminoa* populations, leading us to conclude that our flatworms solely harbour *Amphidinium sp*. Moreover, this photosymbiosis is not obligate as aposymbiotic individuals can survive long-term in our laboratory conditions, albeit with heterotrophic feeding.

Previous literature suggests vertical transmission of photosymbionts in *Waminoa*. Dinoflagellates have been reported within oocytes, egg clutches and recently hatched individuals, leading researchers to hypothesise that maternal transmission is the general mode of action in the genus *Waminoa*.[39,40] However, our observations do not support this generalisation. Our research group never detected dinoflagellates in examined egg clutches, and the resulting juveniles were always aposymbiotic, leading us to question the transmission of symbionts in this strain of *Waminoa*. I hypothesise that aposymbiotic *Waminoa* can integrate *Amphidinium* dinoflagellates as an endosymbiont after exposure to cultured algae or symbiotic donor animals. To test this hypothesis, I utilised a clonal strain of *Waminoa* established in the laboratory (“line C”), previously identified as

Waminoa maja by Sandra Montaño Salazar, through 18S genotyping and phylogenetic analysis. I exposed aposymbiotic *Waminoa* line C flatworms to cultured Amp02 algae and adult symbiotic line C ("donor") flatworms. Additionally, I subjected naturally aposymbiotic juveniles, the offspring of a different clonal line ("line W"), to cultured Amp02 algae. The symbiosis establishment was observed via fluorescent microscopy on living specimens.

1.4. The potential of a defensive photosymbiosis

While the nutritional foundation of marine photosymbioses is well-studied, other aspects remain to be discovered. One understudied facet is the potential defensive role of endosymbiotic microalgae.[41] In so-called defensive symbioses, the symbiont protects its host against threats such as predation and pathogens, often mediated by the production of secondary metabolites.[42] One study provided evidence for a marine defensive photosymbiosis involving symbiotic dinoflagellates, demonstrating the production of anti-inflammatory pseudopterosins by the dinoflagellate *Symbiodiniaceae* residing within the coral host *Pseudopterogorgia spp.*[43] Still, whether this is a more general mechanism of marine photosymbiosis or limited to particular systems is unknown.[44]

Previous reports characterised various polyketides from free-living and isolated symbiotic *Amphidinium sp*. However, whether *Amphidinium* dinoflagellates produce polyketides within the endosymbiosis is unknown. Sandra Montaño Salazar and I hypothesise that Amp02 algae produce multiple polyketides in culture and symbiosis with *Waminoa* line C flatworms. We implemented high-throughput liquid-chromatography tandem mass-spectrometry (HPLC-MS/MS) on extracts from cultured Amp02 algae and symbiotic *Waminoa* line C flatworms to test our hypothesis. Moving forward, a more extensive sample set, including adult aposymbiotic line C flatworms, will be tested to compare cultured algae and symbiotic and aposymbiotic flatworms. Due to time limitations, this thesis reports preliminary results of algae and symbiotic flatworms primarily based on MS1 spectra, i.e. detected masses and their retention times.

1.5. This thesis

In summary, this thesis aims to improve our understanding of the *Waminoa-Amphidinium*

photosymbiosis by first studying the growth of cultured *Amphidinium* Amp02 algae under low- and high-light intensity. Secondly, I am testing different approaches to establish symbiosis in aposymbiotic *Waminoa* flatworms utilising Amp02 algae cultures and symbiotic donor animals. Lastly, Sandra Montaño Salazar and I aim to identify polyketides in cultured and endosymbiotic *Amphidinium* as the initial step of researching the potential of a defensive symbiosis. Overall, this thesis will aid scientific advancements into marine photosymbioses, the foundation of the most biodiverse and productive marine ecosystems – the coral reef.

2. Materials and Methods

2.1. Reagents and solutions

Filtered artificial seawater (FASW): 1,780-1,800 g of sea salt were dissolved in 50 L RO water for 48 h under agitation. The desired salt concentration ranged between 31.5 and 32.5 ppt and was measured using a salinity meter. The artificial seawater was then sterile filtered and stored at 18°C.

IMK medium: per the manufacturer's instructions, 252 mg of Daigo's IMK medium powder (Shiotani M.S. CO., LTD.) were dissolved in 1 L FASW. After sterile filtration, the solution was stored at 4°C and brought to room temperature before use.

CMB: Chloroform, methanol and citrate buffer (0.15 M, pH 4.0 adjusted with 50% liquid NaOH) were mixed in a 1:2:0.8 ratio.

2.2. Organisms

We maintained all organisms in an incubator at 25°C, following a 10:14 h light-dark cycle with a photon flux density (PFD) of 12 μmol m^{-2} s^{-1} unless stated otherwise. Our group's animal care technician, Cátia Pinto, supervises and handles the majority of animal and dinoflagellate care.

Adult *Waminoa*: We kept adult *Waminoa* populations in glass tanks (Ikea 365+ Food Containers, "medium-size" 600 mL square with silicon lid) filled with FASW. Tanks and water were changed weekly. The acoel flatworms were fed with *Artemia salina* shrimp once per week. Experiments using adult flatworms in this thesis used *Waminoa* line C flatworms exclusively, which were collected in 2021 from living corals at the Haus des Meeres in Vienna through the kind collaboration of Daniel Abed-Navandi and have been in clonal laboratory culture since. Genotyping of the 18S region and phylogenetic comparison by Sandra Montaño Salazar identified line C as *Waminoa maja*.

Aposymbiotic adult line C *Waminoa*: Our animal care technician, Cátia Pinto, developed a method to generate aposymbiotic flatworms. Ten adult symbiotic line C flatworms were transferred into a glass tank (Ikea 365+ Food Containers, "small size" 180 mL square with plastic snap lid) filled with 125 mL FASW. The tanks were maintained

in the dark and treated with 0.15 mM menthol twice weekly after water changes for two weeks. Each week, the menthol treatments were stopped for 48 hours. During this time, the flatworms were fed with *Artemia* shrimp one day after changing the tanks. Four weeks after the treatment stopped, the symbiotic status of the flatworms was assessed.

Juvenile *Waminoa:* Juvenile *Waminoa* flatworms used in this thesis were exclusively offspring of *Waminoa* line W, which was collected from corals in a hobby tank in Germany in 2020 and has been in clonal laboratory culture since. *Waminoa* egg patches were removed from the parents' tank, washed with FASW and transferred into new tanks (Ikea 365+ Food Containers, "small size" 180 mL square with plastic snap lid), which were changed along with the FASW twice per week. Tisbe copepods are used to feed juveniles weekly following the protocol of Maegele *et al.*[45] Generally, juvenile *Waminoa* line W could ingest *Artemia* shrimp 40 days after hatching, at which point they were moved to adult care.

Amphidinium gibbosum* strain Amp02*: Amp02 dinoflagellates were previously isolated from a stain of *Waminoa* by Ira Maegele in 2021 and kindly shared with the lab. The *Amphidinium* strain Amp02 was identified as *Amphidinium gibbosum* by Sandra Montaño Salazar, utilising 18S genotyping and phylogenetic comparison. Liquid algae cultures were grown in 1X IMK medium in a plastic cell culture flask with vented lids, filling 10-18% of the flask's total volume. Cultures were split at a typical ratio of 1:5-1:10 every three to four weeks.

2.3. Amp02 dinoflagellate growth dynamics in culture

2.3.1. Dinoflagellate culture

Ten Amp02 dinoflagellate cultures of 18 mL were prepared in 100 mL cell culture flasks with vented lids, each as 1:20 dilutions of an older culture. The initial concentration averaged $1.53 \cdot 10^5 \pm 2.2 \cdot 10^4$ cells/mL. Cultures in low light (L4-L8) were exposed to photon flux densities of 12 μmol m^{-2} s^{-1}, and cultures in high light were exposed to photon flux densities of 230 μmol m^{-2} s^{-1}.

2.3.2. Cell quantification with LUNA cell counter

Twice per week, 100 μL sample aliquots were taken from each culture after mixing for

quantification using the LUNA FX7 automated cell counter (Logos Biosystems). From the aliquots, 10 μL per chamber were loaded into 8-chamber counting slides. Measurements were performed in triplicate per culture. Both fluorescence (FL) and bright-field (BF) cell counting methods were utilised, with FL measurements conducted first to prevent fluorescence signal loss. For fluorescence cell counting, the following settings were used: GF exposure level 0.1; RF exposure level 10; minimum search size 6 μm; maximum search size 60 μm; declumping sensitivity 5; minimum FL intensity 0; minimum roundness 5; dilution factor 1. For bright-field cell counting, the following settings were used: minimum search size 6 μm; maximum search size 60 μm; cell detection sensitivity 6; noise reduction 8; dilution factor 1. BF measurements began only on Day 7 of the experiment.

2.3.3. Statistical evaluation

First, using a two-sided Mann-Whitney U-test, I tested for significant distribution differences between treatments (HLI: high light intensity, LLI: low light intensity) and cell counting techniques (FL: fluorescence, BF: bright-field). For this purpose, I utilised the *wilcox_test* function from the *coin* package in R to calculate exact p-values between the groups presented in Table 1. Ties (identical values) were handled using mid-ranks. Subsequently, p-values were adjusted for multiple testing using the Holm-Bonferroni correction method, implemented with the *p.adjust* function in R set to the method *holm*.

Table 1: For statistical testing, I separated Amp02 algae cell concentration measurements into four groups based on the cell counting technique (BF: bright field or FL: fluorescence) and the irradiance level (HLI: high light intensity or LLI: low light intensity).

Group	Measurement	PFD (μmol m^{-2} s^{-1})	Cultures
BF-HLI	Bright-field	230	H4, H5, H6, H7, H8
BF-LLI	Bright-field	12	L4, L5, L6, L7, L8
FL-HLI	Fluorescence	230	H4, H5, H6, H7, H8
FL-LLI	Fluorescence	12	L4, L5, L6, L7, L8

Growth metrics (maximum specific growth rate μ_{max}, carrying capacity K, and doubling time t_2) were initially predicted by fitting a linear regression model onto the logarithm-

transformed data using the *all_easylinear* function from the *growthrates* package in R. The predicted values were then used as initial parameters for fitting a logistic model with the *all_growthmodels* function from the *growthrates* package in R. Bright-field cell counting was not implemented until day 7, so missing values for days 0 and 3 were substituted with FL measurements.

2.4. Symbiosis establishment

2.4.1. Exposure of aposymbiotic juvenile flatworms to cultured

To test infection in naturally aposymbiotic *Waminoa* line W juveniles, I exposed them to cultured Amp02 algae. Exposure began between 30 and 39 days after the egg patches were laid, about 25-34 days after hatching. Each of nine tanks, containing 4-47 juveniles, received either 20,000 (tanks J1-J5) or 10,000 (tanks J6-J9) algal cells, resulting in algal concentrations of 160 or 80 cells/mL/tank, respectively. The symbiotic status was assessed using fluorescent microscopy as described below. However, the tanks were not changed immediately before imaging, and a maximum of six juveniles per tank were assessed.

2.4.2. Exposure of aposymbiotic flatworms to cultured and symbiotic algae

To examine symbiosis establishment in aposymbiotic adult *Waminoa* line C flatworms, we exposed them to cultured Amp02 dinoflagellates or symbiotic adult line C donor animals. Three adult aposymbiotic *Waminoa* line C flatworms were transferred into each small tank containing 125 mL FASW. For infections with donor animals, a large symbiotic *Waminoa* line C individual was added to each of three tanks containing three small aposymbiotic flatworms (D1-D3), respectively. The negative control tank (D4) included a sizeable aposymbiotic line C flatworm instead of a donor. For infections with cultured Amp02 algae, 10,000 algal cells were added to each of the ten tanks (A1-A10), resulting in an algal concentration of 80 cells/mL/tank. Algae were added weekly, immediately after regular tank and FASW change, for three weeks. Seven negative control tanks (A11-A16) did not receive any algae. During a preliminary experiment, the tanks P1-P3 underwent the same treatment as tanks A1-A10. Table 2 lists the treatment groups from the primary infection experiment using adult *Waminoa* flatworms.

Table 2: Guided symbiosis establishment. Individual tanks of the main experiment with adult *Waminoa* line C are grouped based on their treatment. The control tanks of both experiments were combined.

Group	Measurement	PFD (μmol m^{-2} s^{-1})	Cultures
BF-HLI	Bright-field	230	H4, H5, H6, H7, H8
BF-LLI	Bright-field	12	L4, L5, L6, L7, L8
FL-HLI	Fluorescence	230	H4, H5, H6, H7, H8
FL-LLI	Fluorescence	12	L4, L5, L6, L7, L8

2.4.3. Assessment of infection with fluorescence microscopy

The symbiotic status of each flatworm was assessed weekly using an inverted fluorescent microscope (Leica Thunder Imager DMI8, with an LMD7000 lightbox and DFC9000GT-VSC13724 camera). Before imaging, the animals were transferred into new tanks to avoid residual algal cells in the water, adding 25 mL FASW to limit their movement during imaging. The autofluorescence of the photosynthetic pigments of the algae was visualised using the Cy5 filter cube, with an excitation range of 622-654 nm and emission at 695 nm. Images were acquired with an exposure time of 0.66 s.

Tanks A1-A16 were assessed once weekly for four weeks (weeks 0-3), with no measurements for the negative controls (A11-A16) in week 3. Tanks D1-D3 were checked once per week for three weeks (week 0-2), and D4 was checked once weekly for two weeks (week 0-1) due to technical limitations. Using a stereoscope, I re-evaluated the symbiotic status of D1-D4 on day 40 (week 5). To avoid false positives, *Waminoa* flatworms were classified as infected if more than one algal cell was detected in the host tissue, excluding the gastrointestinal tract. After image acquisition, the tanks were refilled to 125 mL FASW.

2.5. Identification of polyketides

2.5.1. Sample preparation

2.5.1.1. *Waminoa* flatworm samples

The HPLC-MS/MS flatworm samples contained worms from symbiotic *Waminoa* line C, with exact numbers shown in Table 3.

Flatworm sample SW1: The flatworms for sample SW1 were transferred into a 2 mL low-bind plastic tube and washed with 750 mL MilliQ water.

The remaining symbiotic flatworm samples underwent different methods to reduce their salt content.

Salt reduction protocol A: The flatworms for the sample SW3 were transferred into a 2 mL low-bind plastic tube and washed three times with 1 mL FASW. Five washing steps with 1 mL mixtures of FASW and MilliQ water followed, reducing the portion of FASW by 10% with each step to a minimum of 50%. Lastly, the worms were washed twice with 1 mL MilliQ water.

Salt reduction protocol B: The flatworms for the sample SW4 were transferred into a 40 μm mesh sieve (Fisher ThermoScientific) and moved between three wells in a 6-well plate, each containing FASW. They were then moved to a 2 mL low-bind plastic tube and washed twice with 1 mL of FASW / MilliQ water at 60% / 40% and then 50% / 50%. Finally, the worms were washed quickly with 1 mL MilliQ water.

2.5.1.2. *Amphidinium* algae samples

The HPLC-MS/MS dinoflagellate samples contained cells of *Amphidinium* strain Amp02 cultures, with exact numbers shown in Table 3. The original culture was collected in 15 mL sterile plastic tubes and centrifuged twice (2,291 xg, 3 min, room temperature (RT)), removing the supernatant each time. The biomass was collected in a 2 mL low-bind plastic tube, rinsed twice with 1 mL FASW and centrifuged (2,291 xg, 3 min, RT). The resulting pellet was rinsed with 1 mL MilliQ water and centrifuged (2,828 xg, 5 min, RT), discarding the supernatant.

2.5.1.3. *Artemia salina* samples

Artemia salina samples AR1 and AR2 were harvested one day after hatching, with exact

numbers shown in Table 3. The shrimp were transferred into a 40 μm mesh sieve (Fisher ThermoScientific) and passed through four chambers of a 6-well plate, three containing FASW and one filled with MilliQ water. Afterwards, the animals were collected in a 2 mL low-bind plastic tube.

2.5.1.4. Freeze-drying

All samples were frozen at -75°C for a minimum of 72 h before freeze drying (Alpha 1-4 LSCbasic, Martin Christ) for 48 h. The vacuum was set to be 2.6 mbar. The dried biomass was weighed and stored at -20°C until further use.

2.5.2. Extraction protocols

To extract polyketides from the freeze-dried biomass, we utilised two different protocols: a generic lipid extraction protocol provided by Prof Wolfgang Wanek and Rahul Samrat the Division of Terrestrial Ecosystem Research (TER) in CeMESS, University of Vienna, and a methanol extraction protocol specific for amphidinols of *Amphidinium sp.* adjusted from Wellkamp *et al.* 2020.[46]

2.5.2.1. General lipid extraction protocol

The freeze-dried biomass was transferred into 10 mL round-bottom glass vials. After adding 6 mL CMB, the samples were sonicated for 15 min in a sonic bath at RT and vortexed for 30 s. The samples were incubated overnight RT for a minimum of 8 h. The samples were centrifuged (1,386 x*g*, 10 min, RT) and the supernatant was transferred into new 10 mL flat-bottom glass vials. If a pellet remained, 2.6 mL CMB was added to the vial, which was vortexed for 30 s and centrifuged again (1,386 x*g*, 10 min, RT). The supernatant was transferred into the same 10 mL flat-bottom glass vial as before. 1.5 mL chloroform and 1.5 mL citrate buffer (0.15 M, pH 4.0 adjusted with 50% liquid NaOH) were added to the supernatant, vortexed for 30 s and incubated for a minimum of 8 h at RT in the dark. The lipid (lower) phase was transferred to HPLC vials. The extracts were dried at RT under a constant stream of N_2 gas. The dried extracts were stored at -20°C and eluted in 200 μL HPLC-safe methanol before the measurement.

2.5.2.2. Methanol extraction protocol

The following methanol extraction protocol was adapted and modified from Wellkamp *et*

al. 2020 (p. 18, “Extraction of Amphidinols” from strains AA39, AA40, and AA60).[46]

Freeze-dried biomass was dissolved in 500-700 µL HPLC-safe methanol in 2 mL low-bind plastic tubes, depending on the amount of material. After adding 450 mg of Lysing Matrix D (MP Biomedicals), the dried mass was suspended by vortexing. The cells were lysed by reciprocal shaking at maximum speed for 45 s in a FastPrep-24™ bead-beating grinder and lysis system (MPbio) and centrifuged (16,100 x*g*, 10°C, 3 min). The supernatant was collected in a new 1.5 mL low-bind plastic tube. Then 500 µL HPLC-safe methanol was added to the pellet, and the residual matter was lysed by reciprocal shaking at a maximum speed for 5 min in a FastPrep-24™ bead beating grinder and lysis system and centrifuged twice (16,100 xg, 12.9 krpm, 10°C, 3 min). All supernatants were combined, centrifuged (16,100 x*g*, 10°C, 3 min), and moved into a new 1.5 mL low-bind plastic tube. 150 µL of the extract was transferred into the canonical insert of an HPLC vial, capped tightly, and stored at -20°C until further use. The remaining extract was dried for 60 min at 30°C in a rotor evaporator (Eppendorf Concentrator 5301), resuspended in 50 µL HPLC-safe methanol, transferred into canonical inserts of a HPLC glass vial, and stored at -20°C. Before measuring, each extract was filtered with an PTFE syringe filter (0.2 µm pore size, 4 mm diameter; ThermoFisher 42204-NP).

Table 3: HPLC-MS/MS samples, extracted by methanolic or general lipid extraction. The input amount refers to the individual animals for *A. salina* and *Waminoa* samples or the cells for *Amphidinium* samples collected. Sample prepared without specific salt reduction techniques are indicated with “n.a.” in the salt control column.

Sample	Organism	Extraction	Salt control	Input amount	Dry weight
AR1	*A. salina*	Methanolic	n.a.	1,250	1.8 mg
AR2	*A. salina*	Methanolic	n.a.	750	0.8 mg
A1	*Amphidinium*	General	n.a.	$7.75 \cdot 10^6$	85.0 mg
A2	*Amphidinium*	Methanolic	n.a.	$8.25 \cdot 10^6$	9.0 mg
A3	*Amphidinium*	Methanolic	n.a.	$3.21 \cdot 10^6$	8.9 mg

SW1	*Waminoa*	General	n.a.	38	7.3 mg
SW3	*Waminoa*	Methanolic	Protocol A	200	23.6 mg
SW4	*Waminoa*	Methanolic	Protocol B	273	19.5 mg

2.5.3. HPLC-MS/MS

2.5.3.1. Ultimate UHPLC – Orbitrap Q Exactive

The *Amphidinium* extract A1 and the *Waminoa* flatworm extract SW1 were analysed using a platform comprising an UltiMate 3000 UHPLC connected to an Orbitrap Q Exactive (ThermoFisher Scientific). The UHPLC system carried a Water AccQ. Tag Ultra C18 column (2.1 mm x 100 mm, 1.7 μm particles, Milford, MA, USA) coupled to an ACQUITY column in-line guard filter (2.1 mm, 0.2 μm filter, Milford, MA, USA). 5 μL of the extracts were injected for separation at a column temperature of 40°C and a flow rate of 300 μL/min, with two eluents for the gradient elution: eluent A (MilliQ water with 0.1% formic acid) and eluent B (acetonitrile). The per sample runtime was 28 min and followed the gradient in Table 4. The Orbitrap scanned between m/z 100-1500. Negative ionisation was controlled with an automated gain control (AGC) set to 10^6 and an injection time (IT) of 100 ms. Normalised collusion energies of 20%, 40% and 70% for collision-induced dissociation (CID) were used. The dynamic exclusion was set to 2 to detect less abundant ions.

Table 4: Gradient elution for the HPLC-MS/MS using the UltiMate UHPLC – Orbitrap Q Exactive

Time (min)	0	10	15	20	23	24	28
% Eluent B	5	30	50	70	95	5	5

2.5.3.2. UHPLC – HESI Orbitrap

The methanolic extracts AR1 were analysed using a platform comprising a UHPLC connected to a heated electron spray ionisation (HESI) Orbitrap. The UHPLC carried an Acquity Premier HSS T3 column (2.1 mm x 100 mm, 1.8 μm particle size) including a vanguard guard. The sampler had a temperature of 10°C, and 3 μL of the methanolic extracts were injected at a column temperature of 50°C and a flow rate of 400 μL/min, with two eluents used: eluent A (MilliQ water with 0.1% formic acid) and eluent B

(acetonitrile/MilliQ water (95/5, v/v) with 0.1% formic acid). The sample runtime was 24 min and followed the gradient listed in Table 5. The Orbitrap scanned between m/z 200-1500. The sheath gas (Arb.), auxiliary gas (Arb.) and sweep gas (Arb.) of the Orbitrap had flow rates of 60, 10, and 1, respectively. The ion transfer tube had a temperature of 325°C and the vaporiser was heated to 275°C. The measurements were done in negative mode with a spray voltage of -2,500.

Table 5: Gradient elution settings for UPLC-MS/MS using the UHPLC – HESI Obritrap

Time (min)	0	16	22	22.1	24
% Eluent B	25	100	100	25	25

For the MS2, normalised collision energies of 20%, 40% and 70% for collision-induced dissociation (CID) were used. Additional MS1 and MS2 settings are shown in Table 6.

Table 6: MS1 and MS2 settings for HPLC-MS/MS Protocol B

MS1 settings		MS2 settings	
Resolution	60,000	Cycle time	1 s
Scan range	200-1,500	Isolation window	m/z 1.2
Max. Inject. Time	Auto	Resolution	15,000
AGC target	Standard	Normalised AGC target	80%
Microscans	1	Microscans	1
RF Lens	70%	RF Lens	70%

2.5.4. Data analysis and compound prediction

The data generated by the UHPLC-HESI Orbitrap was analysed in collaboration with Valentin Göldner using MZmine software version 4.1.[47] The feature list was aligned across samples, gaps in peaks were filled, duplicates were removed, and the background was subtracted. Moreover, features were filtered based on data points and a Pearson correlation, retaining those with at least five data points and a Pearson correlation coefficient of $r \geq 0{,}85$.

The partition coefficient cLogP of all polyketides from our database was predicted using ChemDraw[48]. The pKa values of polyketide functional groups were predicted in Python

using MolGpKa[49], whereas the average pKa is the average of the functional groups' pKa.

SIRIUS 5, a software for analysing metabolites from tandem mass spectrometry data, was implemented under the guidance of Manuel Uhlir from the Institute of Theoretical Chemistry, University of Vienna, to predict the chemical formula of detected masses based on their fragmentation pattern.

3. Results

3.1. *Amphidinium gibbosum* Amp02 growth

I investigated the growth dynamics of the cultured *A. gibbosum* strain Amp02 algae under two different irradiance conditions to test our hypothesis that exposure to high light intensity promotes growth. To that end, I subjected five Amp02 cultures to low light intensity (LLI, PFD: 12 μmol m^{-2} s^{-1}) and five to high light intensity (HLI, PFD: 230 μmol m^{-2} s^{-1}). The culture density was assessed twice weekly via fluorescence (FL) and bright-field (BF) automated cell counting, whereas only the former was used for the first two measurement days 0 and 3. I split the data into four groups, referring to the light condition (HLI or LLI) and measurement technique (FL or BF). Initially, the cell concentration of all groups increased, peaking on day 28, followed by a decline on day 32. From day 32 to 39, cell abundances increased again, except for HLI cultures measured with fluorescence (FL-HLI), in which cell abundance remained unchanged (Figure 1). In agreement with our hypothesis, HLI cultures had higher cell abundances on days 7-25 ($p < 0.001$). However, this was followed by no significant differences on days 28-35 using the bright-field data. On the last measurement day (39), the densities of LLI-treated cultures were higher ($p < 0.01$).

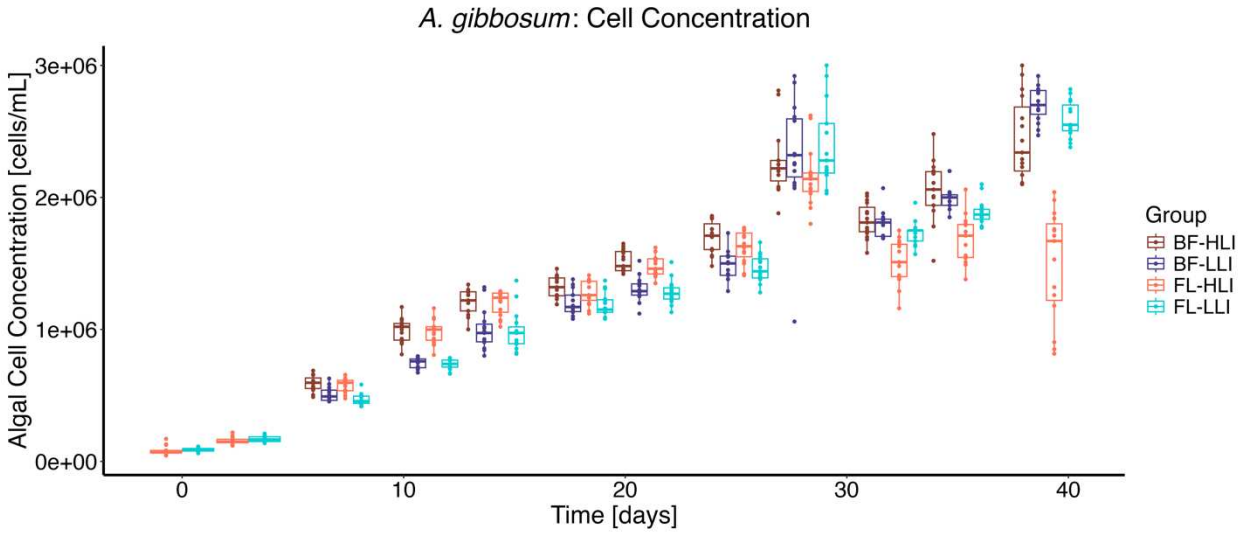

Figure 1: Boxplots of cell concentrations of Amp02 algae in culture under two different light conditions and measured with two automated cell counting techniques (bright field [BF] vs. cell fluorescence [FL]). BF-HLI: Bright field high light intensity, BF-LLI: Bright field low light intensity, FL-HLI: Fluorescence high light intensity, FL-LLI: Fluorescence low light intensity. Days 0 and 3 were only measured with fluorescence. Points represent individual measurements, with each boxplot representing five biological replicate cultures, each measured with three technical repeats.

To identify the exponential growth phase and estimate growth parameters, I first fitted a linear regression model on the logarithm-transformed cell concentration (0.97 ≥

$R^2 \geq 0.92$). The derived exponential fit is shown in Figure 2A. A logistic growth model on the untransformed data ($0.99 \geq R^2 \geq 0.95$), shown in Figure 2B, predicted growth parameters μ_{max}, K and t_2. In doing so, I substituted the missing BF measurements for days 0 and 3 with FL data. According to the linear models, all cultures (H4-H8, L4-L8) exponentially grew between days 0 and 14. In support of our hypothesis that HLI promotes the growth of Amp02 algae, HLI treatment resulted in a higher maximum specific growth rate μ_{max} using both measurement techniques ($p < 0.01$) (Figure 3A, Table 7). Consequently, HLI exposure lead to a faster maximum doubling time t_2 of 2.2-2.4 days compared to LLI with a t_2 of 3.3 days (Table 7). However, when calculating the relative increase of algal cells per day, HLI cultures grew faster than LLI cultures until day 11, after which LLI cultures proliferated faster. As this behaviour is also reflected in the cell abundances, I conclude that HLI exposure initially promotes the growth of *Amphidinium gibbosum* strain Amp02, with the growth rate declining 11 days after inoculation, resulting in a lower cell concentration on day 39 compared to LLI cultures.

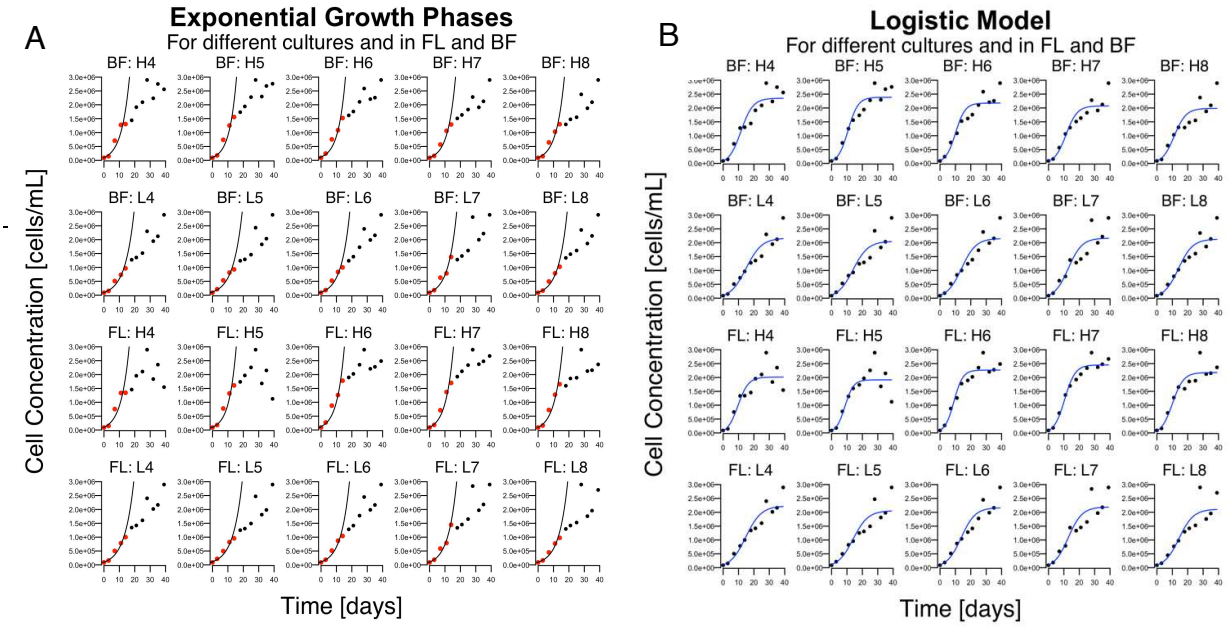

Figure 2: Growth models for the 10 cultures of Amp02 algae shown in Figure 1. Cultures H4-H8 were exposed to high light intensity. Cultures L4-L8 were exposed to low light intensity. "BF" indicates bright field measurements and "FL indicates fluorescence measurements from automated cell counting. Points show the average of three technical repeats per culture. A) A linear model was fitted onto the logarithm-transformed data to identify the exponential growth phase. The model was adjusted to show exponential growth (black line). Red data points indicate measurements predicted to be undergoing exponential growth. B) A logistic growth model (blue line) was fitted onto the untransformed data.

Table 7: Growth parameters of Amp02 algae cultures. Groups refer to the light conditions (HLI or LLI) and the automated cell counting technique (BF or FL). The growth parameters of each group are the average of 5 biological replicate cultures, each measured with three technical repeats.

Group	μ_{max} (d^{-1})	t_2 (d)	K (cells/mL)
BF-HLI	0.284	2.44	1904927
BF-LLI	0.211	3.28	1997328
FL-HLI	0.314	2.21	1605793
FL-LLI	0.211	3.28	1950356

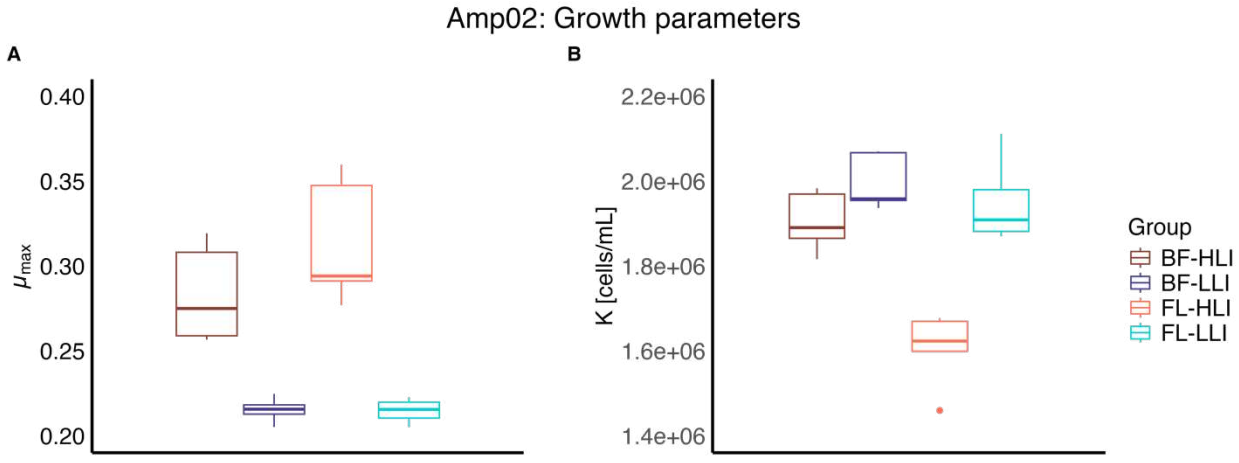

Figure 3: Amp02 algae growth parameters under two different irradiance conditions and measured with bright field or fluorescence based automated cell counting. BF-HLI: Bright field high light intensity, BF-LLI: Bright field low light intensity, FL-HLI: fluorescence high light intensity, FL-LLI: fluorescence low light intensity. A) Boxplots of the maximum specific growth rate μ_{max}. B) Boxplots of the carrying capacity K. Points demonstrate outlier values.

I additionally observed that between days 32 and 39, BF counts detected significantly more cells in HLI samples than FL measurements ($p < 0.001$) (Figure 1), which indicates cell bleaching under this condition. This trend is reflected in the carrying capacity, as only HLI-treated flasks counted by fluorescence have a significantly lower carrying capacity ($p < 0.1$) (Figure 3B, Table 7). Visual inspection of the microscopy pictures from the LUNA automated cell counter confirmed the inability of the FL method to count these cells: many that were detected in the BF counts remained undetected in FL counts (Figure 4). The discrepancy between FL and BF measurements stemmed from a decreased fluorescent signal from the loss of autofluorescent photosynthetic pigments, i.e. bleaching, under HLI

exposure.

Another discrepancy between FL and BF counts was observed for LLI cultures on day 35 ($p < 0.5$). Visual inspection revealed that it was not due to decreased fluorescent signals of the cells but to higher amounts of non-fluorescent cell debris, which the LUNA automated cell counter identified as cells using the BF method. These results demonstrate that exposure to high light intensity (PFD: 230 μmol m^{-2} s^{-1}) increases growth rates in *Amphidinium* Amp02 liquid cultures for nearly two weeks. Yet, after four weeks, the high light intensity causes Amp02 algae to lose fluorescent signals and thus bleach.

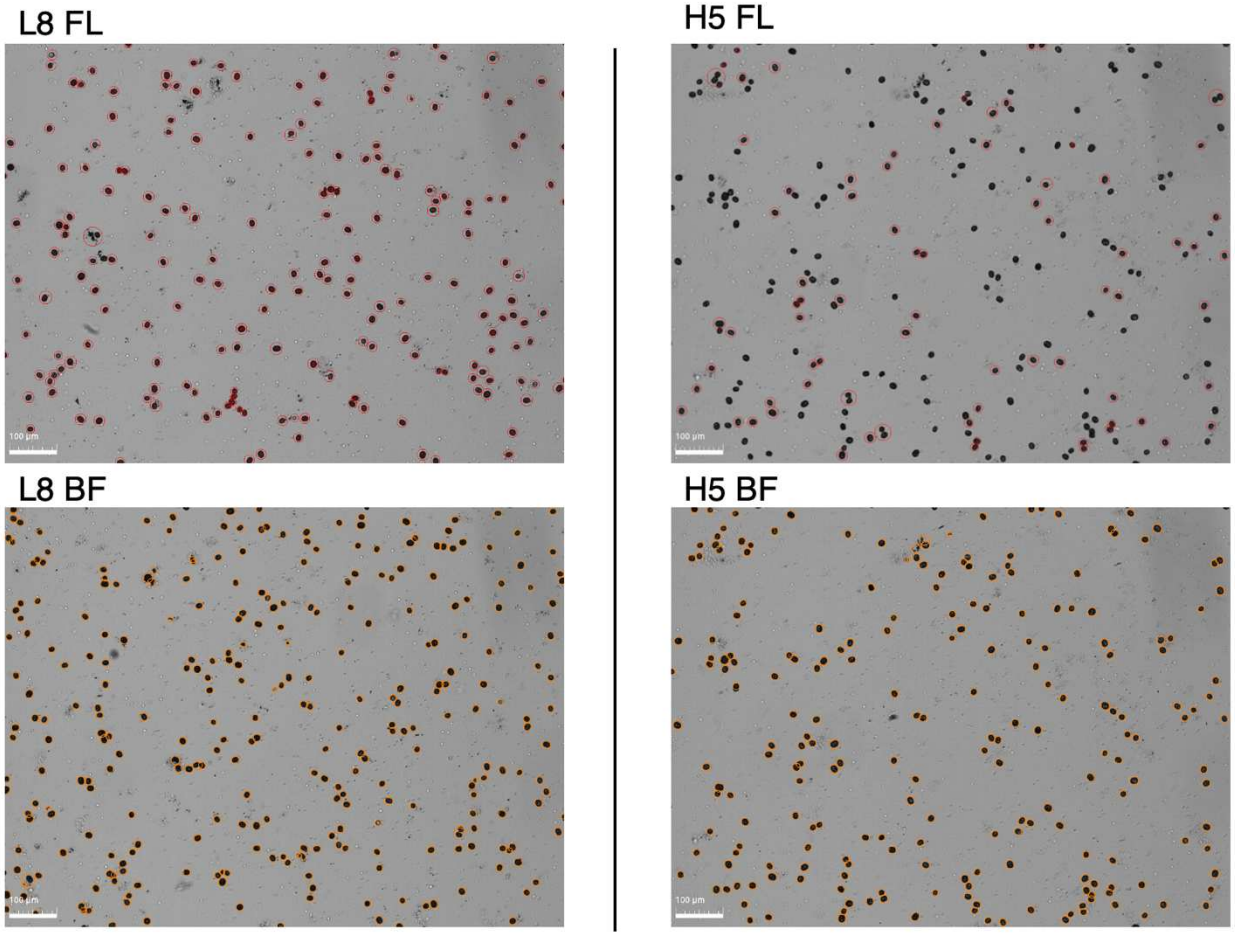

Figure 4: Microscopy pictures of measurements of Amp02 algae cells from the LUNA automated cell counter taken on day 39. Lefthand panels show cell detection in one of the LLI-treated replicate cultures, flask L8, using fluorescent (L8 FL) or bight field automated cell counting (L8 BF). Righthand panels show cell detection in a HLI-treated flask H5 counted with fluorescence (H5 FL) or bight field (H5 BF). In all panels, cells identified by the technique and included in the counts by the LUNA automated cell counter are circled in red or orange. White bars: 100 μm.

3.2. Symbiosis establishment

Previous reports from Bucher *et al.* and Hambleton *et al.* demonstrated that adult and juvenile *Aiptasia* sea anemones can integrate compatible *Symbiodinium* dinoflagellates algae as endosymbionts from the environment.[50,51] Based on this, I hypothesised that the exposure to cultured algae alone, as well as exposure to symbiotic *Waminoa* flatworms ("donors"), would result in the formation of a stable symbiosis. To test this hypothesis, I conducted experiments with adult and juvenile aposymbiotic *Waminoa* flatworms, with juvenile flatworms being exposed only to cultured algae and not to symbiotic "donors". A schematic overview of the experimental design is shown in Figure 5.

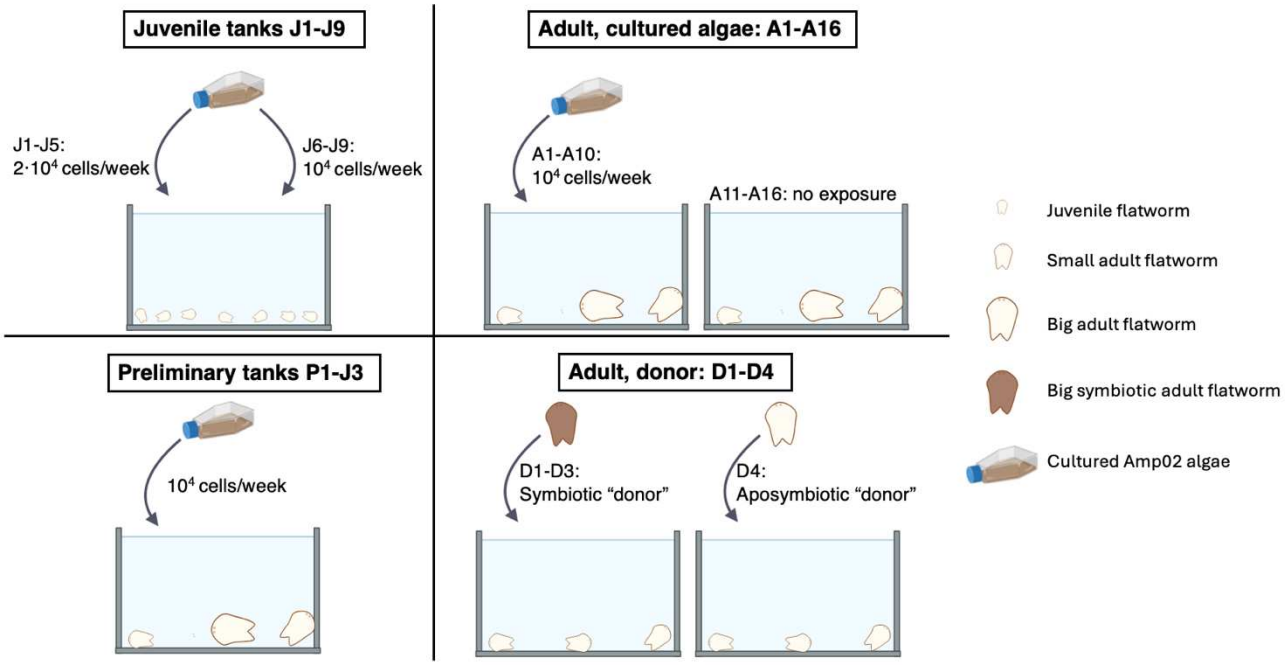

Figure 5: Schematic overview of symbiosis establishment experiments. Created in BioRender.com[52]

Flatworms with at least two algal cells within their tissue were classified as symbiotic for this thesis. To avoid false positives, Amp02 algae detected within the syncytial cavity of the flatworms were excluded from the count because it was ambiguous whether these algal cells were endosymbiotic.

3.2.1. Establishing a workflow

To establish an effective workflow, I conducted a preliminary experiment. Each week, I added 10,000 *Amphidinium gibbosum* strain Amp02 cells to each of three tanks (preliminary tanks P1-P3), each containing three adult aposymbiotic *Waminoa* line C

flatworms (Figure 5). I monitored the flatworms through weekly fluorescent microscopy. However, I imaged a maximum of seven worms per tank instead of assessing all flatworms within a tank. Despite observing many algal cells within the flatworms, the worms retained a white body colouration throughout and after the three-week exposure to Amp02 algae, indicating they remained aposymbiotic. While most flatworms appeared to have some internal symbionts, the positioning of algal cells within the worm's tissue during worm movement made distinguishing between true and false positives difficult.

While most animals appeared to have internal symbionts, the algal cells appeared in different positions within the tissue when the worms moved, whereby it was difficult to distinguish between true and false positives. This issue occurred because of free-floating algal cells surrounding the worms. Additionally, the worms' movement made imaging difficult. During the primary experiments, I addressed these issues by changing the water immediately before imaging to remove algal cells from the water and by reducing the tanks volume from 125 mL to 25 mL of FASW during imaging to limit the worms' movement. These adjustments made the observations more accurate.

3.2.2. Symbiosis establishment of juvenile flatworms with cultured Amp02 algae

To investigate whether naturally aposymbiotic juvenile *Waminoa* line W can take up dinoflagellates from the environment to establish a stable endosymbiosis, I exposed nine tanks containing between 4-47 worms to cultured Amp02 algae. Once per week, juvenile tanks J1-J5 were exposed to 20,000 algal cells per tank, and juvenile flatworm tanks J6-J9 were exposed to 10,000 algal cells per tank. I reduced the amount of algal cells after observing that all worms in tanks J1 and J4 died within three and one week of exposure, respectively.

In tank J7, one symbiotic worm was identified that contained three and two algal cells 63 and 84 days after the treatment started. However, the remaining juvenile flatworms in all tanks remained aposymbiotic. Notably, a faint fluorescent signal was frequently detected in the gastrointestinal tract of the juvenile flatworms, suggesting that they ingested and possibly digested the dinoflagellates.

3.2.3. Symbiosis establishment of adult aposymbiotic *Waminoa* flatworms

To investigate our ability to control symbiosis establishment in adult *Waminoa*, I exposed adult aposymbiotic line C flatworms to cultured *Amphidinium gibbosum* strain Amp02 (tanks A1-A10) or symbiotic *Waminoa* line C donors (tanks D1-D3). Negative control

tanks either received no treatment (A11-A16) or were exposed to a large aposymbiotic *Waminoa* line C flatworm (D4). I monitored all flatworms of a tank, primarily through weekly fluorescent microscopy.

3.2.3.1. Symbiosis establishment with cultured Amp02 algae

Contrarily to my hypothesis that adult aposymbiotic flatworms can form a stable endosymbiosis in the presence of algal cells free-floating in the surrounding seawater, I only observed transient association of *Waminoa* line C exposed to cultured dinoflagellates. After two weeks, I detected five algal cells in the tissue of one flatworm in the tank A5, whereas the remaining population stayed aposymbiotic. The next week, tanks A1 and A7 contained one infected flatworm each, carrying 35 and 20 algal cells, respectively (Figure 6). However, at that timepoints tank A5 no longer held any symbiotic worms anymore. After discontinuing the algae exposure, the worms in tanks A1 and A7 no longer contained detectable algae, and all populations remained aposymbiotic, having a white body colouration. As the flatworm population size of tanks A1, A5 and A7 increased after detecting the symbiotic worm (Figure 8), it is reasonable to assume that the endosymbiotic dinoflagellates were rejected.

3.2.3.2. Symbiosis establishment with symbiotic donors

Symbiosis establishment using symbiotic donors, on the other hand, resulted in a stable, long-term endosymbiosis. After one week, only a single flatworm (tank D1) carried two algal cells in its tissue. One week later, five out of six initially aposymbiotic worms hosted symbionts (3, 4, 7, 10 and 30 algal cells, respectively) (Figure 6). Due to technical difficulties, I could no longer use the fluorescent microscope, thus missing data for weeks two and three. Nonetheless, stable endosymbiosis was established: on day 40, all flatworms appeared either light- or dark-brown, indicating recently infected worms or longer symbiosis, respectively (Figure 7). On day 45, after exposure to the donor worms, the colouration of recently symbiotic worms intensified, whereby distinguishing them from donor animals was no longer possible.

Thus, I conclude that *Waminoa* line C aposymbionts form stable associations with dinoflagellates when exposed to symbiotic line C donor flatworms but not to cultured Amp02 dinoflagellates alone

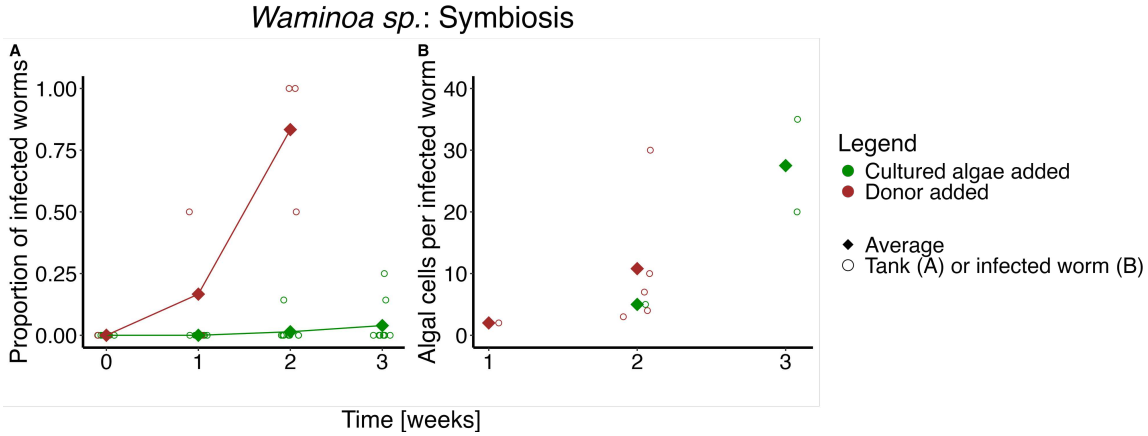

Figure 6: Symbiotic status of *Waminoa sp.* line C aposymbiotic adults after exposure to cultured Amp02 algae (green) or to symbiotic line C "donor" worms (red). A) The relative proportion of infected worms in all tanks of the same treatment. B) The number of algal cells per infected worm, in the host tissue and not the gastrointestinal tract. Open circles show values per tank (A) or worm (B), and diamond show the averages of all values per treatment.

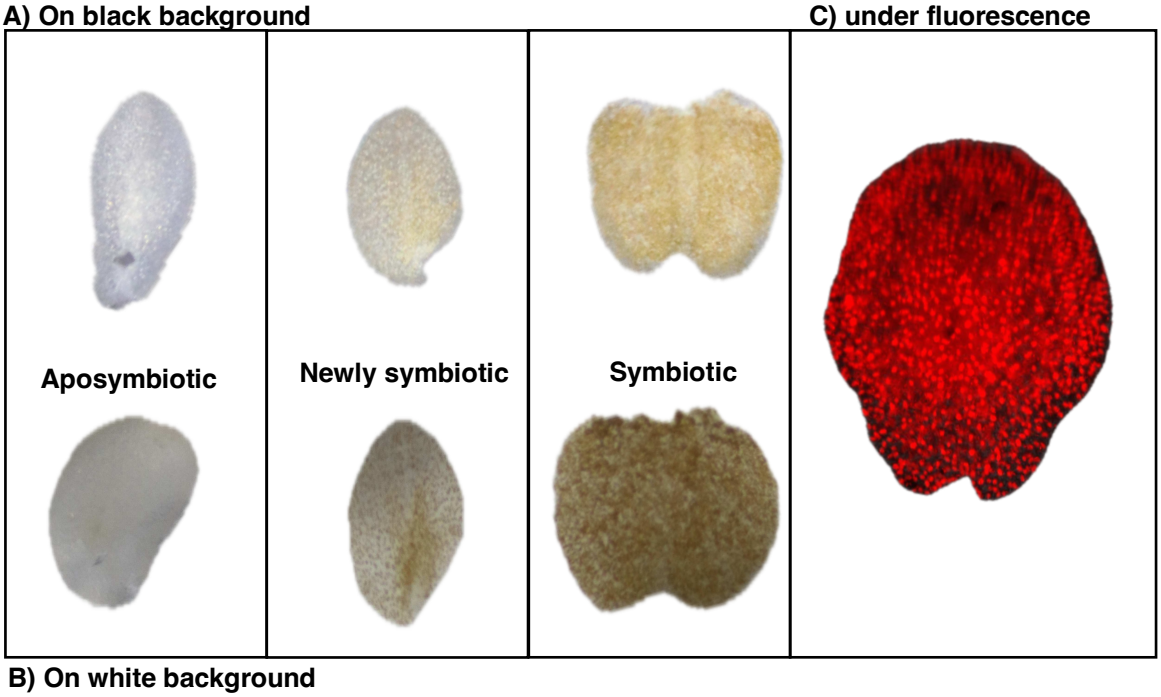

Figure 7: *Waminoa sp.* line C in different symbiotic stages. The pictures were taken via a stereoscope (4x magnification) on day 40 of the symbiosis establishment with donor animals (tanks D1-D4). Animal sizes relative to one another remain unchanged in panels A, and B. Aposymbiotic worms (tank D4) have a white body colouration. Newly symbiotic flatworms have a light brown body colour. A) and B) show the same worms with the pictures taken on a black background (A) or a white background (B). C) An overlay of a fluorescent and bright-field microscopy picture of a fully symbiotic worm. Cells that contain symbiotic dinoflagellates fluoresce in red.

3.2.4. *Waminoa* population dynamics

Besides the symbiosis establishment, I was interested in how the treatments affected population sizes since *Waminoa* flatworms can reproduce asexually through splitting, on

the order of days to weeks. *Waminoa* flatworms exposed to cultured Amp02 algae, as well as the control group (no exposure), showed a slow increase in population size over the three-week experiment, with no significant differences between groups (Figure 8).

The population sizes of tanks D1-D3 were bigger when donor animals were included in the count, as these worms were primarily asexually reproduced (Figure 8A). However, the population of aposymbionts was much smaller: they decreased in tanks D1-D3 over the first two weeks, and on day 13, each tank contained two aposymbiotic flatworms compared to the three at the beginning of the experiment (Figure 8B). One week later, disambiguating donors from aposymbiont "receiver" worms became more difficult, as most animals had similar body sizes and started to appear in different shades of white to brown as symbiosis became established in the latter group (Figure 7). Still, aposymbiont "receiver" worms seemingly started to asexually reproduce as symbiosis establishment proceeded The number of small white to light-brown animals increased to 3-7 animals per tank. However, these are estimates, and the number of newly symbiotic worms may vary around these values.

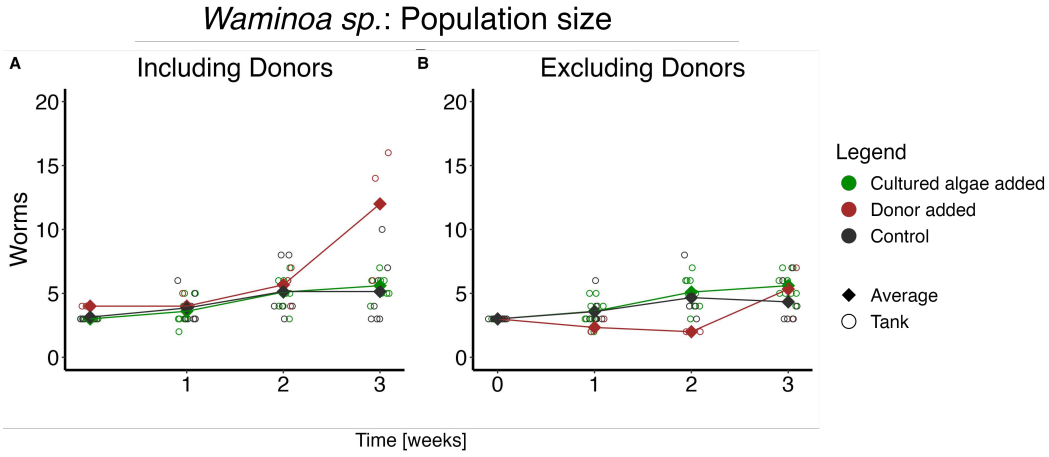

Figure 8: *Waminoa* population dynamics when exposed to cultured Amp02 algae (with algae, green) or symbiotic donor animals (with donor, red). The negative control is shown in black. Unfilled dots show the population size of individual tanks. Diamonds connected by lines indicate the average population size for all tanks of one treatment.

Taken together, exposure to donor animals limited population growth during the first two weeks, after which the newly symbiotic worms began to multiply, whereas exposure to Amp02 algae from cultures did not affect population sizes compared to controls.

3.3. Identification of polyketides

The primary objective of these experiments was to identify polyketides in cultured *Amphidinium gibbosum* strain Amp02 dinoflagellates and in symbiotic *Waminoa* line C flatworms hosting Amp02 dinoflagellates using high-performance liquid chromatography (HPLC) tandem mass spectrometry (MS/MS). Sandra Montaño Salazar and I hypothesised that Amp02 dinoflagellates produce polyketides in culture and symbiosis, thus, expecting to find polyketides in both cases, although these might differ in polyketide identity and amount. Due to logistical and time constraints, this thesis only reports preliminary results primarily based on MS1 information. The main issue was the lack of reference fragmentation spectra to compare to putatively, wherethrough definite identification was not possible. Future experiments aim to overcome this challenge and will analyse a larger sample set including samples of aposymbiotic flatworms.

3.3.1. Polyketide database

Initially, we compiled a list of 116 literature reported polyketides produced by *Amphidinium* species. MS2 fragmentation patterns have been published for 39 polyketides, with 20 performed in negative ionisation mode. We obtained the monoisotopic mass, chemical formula, and SMILES from the databases PubChem[53], ChemSpider[54], or J-Global[55]. However, 16 of the 116 compounds did not have entries in any of these databases, which limited our ability to include them in the following analysis.

3.3.2. Salt reduction

Given that all our organisms are marine, it was essential to reduce the salt content in the samples before freeze-drying, as high sodium chloride levels are known to suppress signal intensity during mass spectrometry.[56,57] We prepared samples of cultured Amp02 algae (A2, A3), symbiotic *Waminoa* line C worms (SW3, SW4), and *Artemia salina* shrimp (AR1, AR2), the flatworms' food (Table 3). To minimise contaminations from *A. salina* in *Waminoa* samples, we only used line C flatworms at least six days post-feeding, to ensure all food was completely digested. We employed simple MilliQ water washing protocols for Amp02 dinoflagellate and *A. salina* samples to reduce the salt content.

In contrast, salt reduction in the flatworm samples proved more challenging. *Waminoa* worms exposed to MilliQ water, i.e. low osmotic pressure, are fragile and during agitation, many worms disintegrated. To address this issue, we implemented two intermediate washing steps using mixtures of MilliQ water and filtered artificial seawater (FASW) in

small sample tubes. During these steps, the flatworms were alive but lost their ability to attach to the plastic sample tube, instead clumping into a ball-like structure. Removing the liquid during subsequent washing with MilliQ water was more manageable, as it was easier to avoid pipetting the worms.

We evaluated two highly similar salt reduction protocols, which only differed in the number of intermediate washing steps. Moving forward, we will continue with Salt Reduction Protocol B, which includes two instead of five intermediate washing steps with 60% and 50% FASW in MilliQ water. This protocol involves fewer steps, reducing the time the flatworms are exposed to low osmotic pressure.

3.3.3. Extraction

After reducing the salt content and freeze-drying the samples, we initially employed a generic lipid extraction protocol provided by Prof. Wolfgang Wanek and Rahul from the Division of Terrestrial Ecosystem Research (TER) in CeMESS, University of Vienna. However, this method was inefficient for concentrating putative polyketides. HPLC-MS/MS analysis revealed masses that could correspond to polyketides, but the concentrations were so low that they might have been background noise. Additionally, technical issues with the equipment further hindered the process, leading us to abandon this method.

Consequently, we adopted and modified a methanol-based protocol, originally developed by Wellkamp *et al.*, specifically designed for extracting amphidinols – a type of polyketide from *Amphidinium* species.[46] Additionally, methanol aids in salt reduction due to sodium chloride's low solubility in methanol (1.375% w/w).[58]

3.3.4. HRES-HPLC-MS/MS analysis

In collaboration with Valentin Göldner from the division of Environmental Geosciences (EDGE) at the CeMESS, University of Vienna, we analysed eight methanolic extracts using HRES-HPLC-MS/MS in negative ionisation mode. We processed the measurements with MZmine (software version 4.10).[47] The samples are listed in Table 3 and include one dinophysistoxin 1 standard, two blanks (B01, BE1), two *Artemia salina* samples (AR1, AR2), two Amp02 dinoflagellate samples (A2, A3), and two symbiotic line C flatworm samples (SW3, SW4).

We identified 69 masses with different retention times (rt) that matched $[M-H]^-$ or $[2M-H]^-$ adducts of 18 known polyketides produced by *Amphidinium sp.* Table 8 lists all

polyketides that matched detected masses, indicates in which samples they were found, and provides predicted chemical properties. More information regarding the results of the HPLC-MS/MS analysis can be found in Table 10, Appendix. As expected, the standard contained two masses that matched dinophysistoxin 1, most likely isotopes of each other. A mass matching amphidinolide M was detected in all samples that underwent methanol extraction, including the blanks (B01, BE1). We attribute this mass to contamination, likely from plastic materials used during the extraction process. The symbiotic worm samples SW3 and SW4 had the most MS1 matches to polyketide masses with 51 and 48 matches, respectively. Dinoflagellate samples A2 had 20 and A3 had 14 matches. *Artemia salina* samples AR1 and AR2 had 7 and 5 matches, respectively. This distribution can be partially explained by the sample complexity, since flatworms harbour many different microbial species, while dinoflagellate samples came from cultures, which are contaminated but most likely have a lower microbial diversity. *Artemia salina* samples, on the other hand, should also carry a diverse community of microbes as they are not kept in sterile conditions, whereby in this case the lower detection rate cannot be explained by complexity.

We planned to compare the fragmentation patterns of each match to literature-reported negative electron spray mode (ES-) MS2 spectra; however, none were available in the literature, and these compounds are also not commercially available. Without fragmentation pattern comparison, we cannot identify whether the detected masses truly represent polyketides or other metabolites with the same monoisotopic mass, which is very likely. Still, we employed other methods to improve our confidence in the results. While these methods are not able to identify the detected masses, they can slightly improve our confidence and will be implemented in future analyses.

3.3.5. Ionisation and pKa

Among other factors, the pKa indicates how ionisable a compound or a functional group is. We implemented MolGpKa[49] to identify the pKa values of polyketides with database entries, which are listed in Table 9 in the Appendix. The predicted pKa values of putatively detected polyketides are also listed in Table 8. The average pKa of a molecule is the average of the pKa values of its functional groups. The pKa of Amphidinoketide I and II and Amphidinolide X could not be predicted using this method, as they do not possess any functional groups with acidic or basic characteristics. The remaining 97 polyketides primarily contain ketones, aliphatic and phenolic alcohols, while carboxylic and sulfonic

acids are less abundant. Except for Amphidinin B (average pKa = 4.34), the molecules have very weak acidic characteristics with average pKa values over ten (Table 9, Appendix). This points towards a low ionisation efficiency since especially alcohol and ketone functional groups are difficult to deprotonate.[56]

3.3.6. Lipophilicity

To estimate the solubility of polyketides in methanol, we calculated the cLogP of the 100 polyketides with database entries using ChemDraw[48]. The partition coefficient P between *n*-octanol and water is a parameter for lipophilicity. Typically expressed in its logarithmic form, LogP, it can be experimentally determined or theoretically calculated (cLogP). Positive LogP values indicate lipophilicity, while negative values indicate hydrophilicity.[59] For effective extraction, the LogP values of the compounds and methanol (cLogP =-0.764) should be similar to ensure sufficient solubility.[60] The cLogP values of polyketides with database entries vary significantly, ranging from -13.913 to 6.604 (Table 9, Appendix). Polyketide groups with a negative cLogP (hydrophilic) from our database include amdigenols, amphezonols, amphidinols, carteraols, karatungiols, luteophanols, symbiopolyol, and amphidinolide N. Polyketides groups with a positive cLogP (lipophilic) from our database include amphidinins, amphidinoketides, amphidinolactones, the remaining amphidinolides, amphirionins, aolopsinols, iriomoteolide, and lingshuiols. These groupings are specific to the polyketides from our database and cannot be generalised. Methanol, which is slightly hydrophilic, is suitable for extracting several polyketide groups, but its use could limit the extraction efficacy for very hydrophilic or very hydrophobic polyketides.

The polyketides that matched detected peaks in their exact mass all have positive cLogP values ranging from 0.76 to 4.32 (Table 8). These values suggest that the compounds are more lipophilic than methanol, which argues against their detection. However, it is important to note that the cLogP has limitation and does not offer definite predictions regarding solubility.

Moreover, the cLogP correlates with the retention time of compounds as more hydrophilic molecules tend to have a shorter retention time. Figure 9 shows that the predicted partition coefficient of most masses associated with polyketides and the measured retention time did not correlate well in a linear regression model. Only 12 out of 69 detected masses fell into the 95% confidence interval. However, this method has limits as multiple other structural and physiochemical properties influence the retention time.[61]

Furthermore, the standard dinophysistoxin 1 did not fall into the 95% confidence interval, casting doubt on the validity of this model. Yet with this caveat in mind, this model could be expanded on to include other chemical properties and be used together with other analyses to shed light on the data.

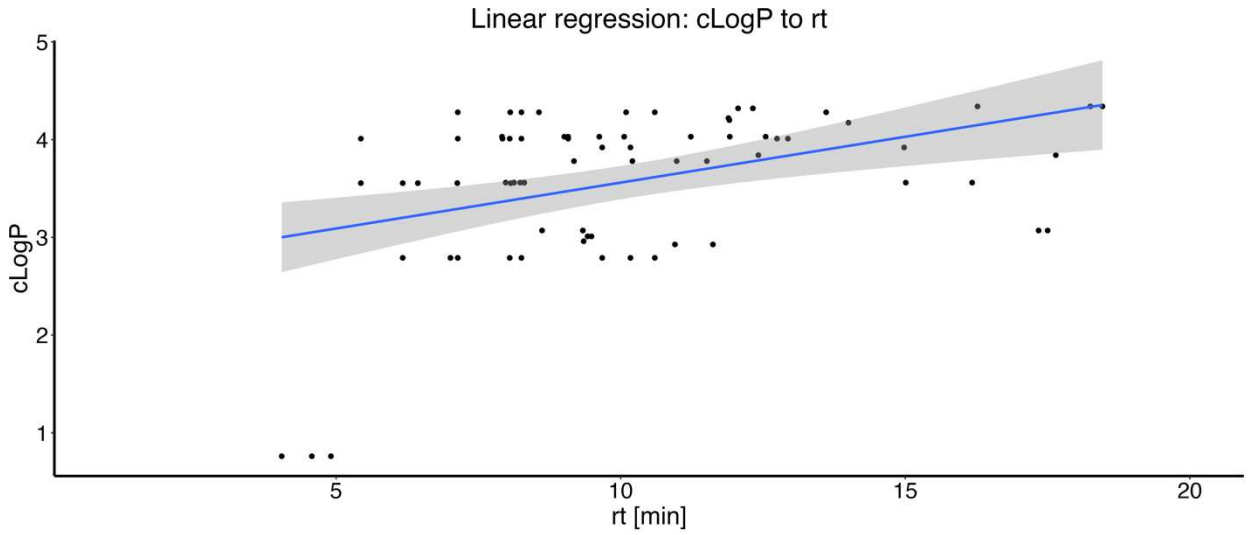

Figure 9: Linear regression of the predicted cLogP of putatively detected polyketides to the measured retention time (rt) in minutes of their corresponding masses. The blue line represents the linear regression model with the 95% interval indicated by the shaded area. Individuals dots represent measured retention times.

Additionally, we predicted the molecular formula of polyketide annotated masses based on the MS2 spectrum using the Sirius Software[62], with guidance from Manuel Uhlir from the Institute of Theoretical Chemistry at the University of Vienna. Sirius provides the parameter explained intensity (eI) to indicate the confidence level for peak annotation. The explained intensity is the ratio of the intensity of annotated peaks to the total intensity, with each peak corresponding to an MS2 fragment. We only regarded explained intensities of over 80% to be sufficiently confident. With that in mind, 48 of the Sirius-predicted molecular formulas matched the formula of the associated polyketides, whereas five could not be predicted, and the remaining 18 did not match or had an insufficient eI (Table 8).

Despite questioning the validity of the linear regression, we report that four masses fell within the 95% confidence interval of the model, and their Sirius-predicted chemical formulas matched the annotated polyketide with an explained intensity of over 80%. Additionally, these masses had a difference between the detected and monoisotopic mass of below 0.5 ppm with our original cutoff set at 5 ppm. Among them are two masses

corresponding to amphidinolide A (1. m/z = 529.31686, rt = 10.9847 min, eI = 98.6% and 2. m/z = 529.31692, rt = 11.5151 min, eI = 96.8%), one mass corresponding to amphidinolide C (m/z = 713.42728, rt = 12.4198 min, eI = 83.6%), and one mass corresponding to iriomoteolide 1a/1b (m/z = 505.31696, rt = 8.0686 min, eI = 97.1%). Excitingly, the masses corresponding to amphidinolide A and iriomoteolide 1a/1b were only detected in the symbiotic worm samples SW3 and SW4, while amphidinolide C was also found in both algal samples.

However, the corresponding polyketides are all lipophilic and have high average pKa values (Table 8), which limits their solubility in methanol. Additionally their functional groups are difficult to deprotonate, speaking against their detection. In the end, only reference fragmentation patterns from MS2 spectra of the isolated compounds can truly identify the detected masses.[61] Still, we cannot dismiss the possibility that the detected masses are polyketides and will disambiguate their identity in future analyses.

Overall, this experiment showed limitations of the current workflow, which will be addressed moving forwards. Moreover, it gave a first insight into the possibility that dinoflagellates produce toxic secondary metabolites within their symbiotic host and while the results are not trustworthy yet, they will be compared to future experiments, aiding the analysis.

Table 8: Information on putatively detected polyketides. Names in bold indicate those that were predicted with a slightly higher confidence by the cLogP linear regression and the Sirius Software (see text). "/" in the names of annotated polyketides indicates several compounds with the same exact mass and chemical formula. The cLogP is the partition coefficient between *n*-octanol and water, and was predicted by ChemDraw. The pKa is the mean pKa of all functional groups of the molecule and was predicted by MolGpKa – a graph convolution neural network. *Amphidinolide X did not contain any functional groups that can be used for pKa prediction. NM refers to the number of masses that match each annotated polyketide. The sample column lists all samples that contained at least one NM of the annotated polyketide. "Shrimp": *Artemia salina* shrimp as worm food, samples: AR1 and AR2; "Algae" *Amphidinium gibbosum* strain Amp02 in liquid culture, samples: A2 and A3; "Worms": symbiotic adults of *Waminoa* line C flatworms, samples: SW3 and SW4; "Standard": Dinophysistoxin 1 (see Table 3 about these samples)

Annotated polyketide	cLogP	pKa	NM	NM eI > 80%	Samples
Amphidinin A	4.32	13.75	2	2	AR1, A2, A3, SW3, SW4
Amphidinolactone A	3.56	13.22	6	0	AR1, AR2, A2, A3
Amphidinolide A	3.78	13.20	4	4	SW3, SW4
Amphidinolide B/B1/D	2.79	12.90	8	7	SW3, SW4

Amphidinolide B4/B5/B7	4.03	12.94	8	8	SW3, SW4
Amphidinolide C	3.84	12.91	2	1	A2, A3, SW3, SW4
Amphidinolide K	3.92	13.82	3	2	A2, A3, SW3, SW4
Amphidinolide M	4.17	13.70	1	0	B01, BE1, AR1, AR2 A2, A3, SW3, SW4
Amphidinolide N	0.76	11.70	3	1	SW3, SW4
Amphidinolide P	3.01	12	2	0	A2, A3
Amphidinolide Q	4.34	12.48	3	0	A2, A3
Amphidinolide T1/T3-T5	4.22	12.89	1	0	A2
Amphidinolide X	4.01	NA*	8	7	A2, A3, SW3, SW4
Amphidinolide Y	2.96	13.08	1	1	SW4
Iriometeolide 1a/1b	3.56	12.05/ 12.24	5	2	SW3, SW4
Iriomoteolide 12a	4.2	12.47	1	0	A2
Iriomoteolide 1c	4.28	12.06	7	7	SW3, SW4
Iriomoteolide 3a	3.07	13.41	4	1	A2, A3, SW3
Dinophysistoxin 1	2.93	10.41	2	2	Standard

4. Discussion

4.1. *Amphidinium gibbosum* algae growth dynamics

By monitoring the growth dynamics of *Amphidinium gibbosum* strain Amp02 under two light conditions, I demonstrated that high light intensity (HLI) significantly boosts the growth rate for the first week of exposure. This initial surge resulted in higher cell concentrations between days 7-25. However, by day 11, the growth rate of HLI cultures decreased. By days 28 to 35, cell densities in both treatments had equalised. Notably, by day 39, the cell density of the low light intensity (LLI) cultures surpassed that of the HLI cultures.

The initial increase in growth rate under HLI aligns with previous findings, which demonstrated that enhanced light availability stimulates the growth of marine and freshwater phytoplankton.[23,63] Duo *et al.* proposed that microalgal species thrive within an optimal range of light intensity and nutrient concentration, which promotes growth rate and bloom formation; exceeding or falling short of these conditions impedes growth.[64]

Nutrient limitation is unlikely to have caused the reduced growth rate in HLI cultures from day 11 onwards because all cultures were grown in the same minimal media and had similar starting concentrations, averaging $1.53 \cdot 10^5 \pm 2.2 \cdot 10^4$ cells/mL, a relatively dilute amount. Moreover, the population size increased until day 28, suggesting sufficient nutrient availability during this time.

Consequently, photoinhibition is one plausible explanation for the reduced growth rate after day 7, implying that the chosen HLI exceeds the optimal irradiance level of Amp02 dinoflagellates. The irradiance optimum I_{opt} of the closely related species *Amphidinium carterae* was predicted to be 69.5 μmol m^{-2} s^{-1}.[65] Hence, the HLI conditions in my experiment, at 230 μmol m^{-2} s^{-1}, would be above the optimum.[65,66] Still, taxonomy and I_{opt} do not seem to correlate in most marine phytoplankton, including dinoflagellates, and thus, I do not know the optimal irradiance level of Amp02 algae specifically.[65] High visible or UV radiation promotes the production of reactive oxygen species (ROS).[67] HLI might lead to the accumulation of ROS over time, as previously reported by Rodríguez *et al.*[68] The build-up of oxidative stress as the culture ages would explain why the growth rates of HLI cultures declined further into the experiment. On the other hand, the LLI cultures would not experience as much oxidative stress, leading to a slower but steady increase in cell density. In addition, the accumulation of ROS in HLI cultures putatively led to cell

bleaching observed from day 32 onwards. Bleaching suggests the degradation of photosynthetic pigments likely caused by an interplay of *A. gibbosum* adapting to high visible light radiation and a possible increase in oxidative stress.[69]

Our data additionally indicates that the chosen LLI is below the optimum of Amp02 dinoflagellates. The growth rate of microalgae is maximised at the irradiance optimum when disregarding other environmental factors. Still, the maximum growth rate of HLI cultures was initially higher than under LLI treatments, suggesting that the I_{opt} of Amp02 algae lies between photon flux densities of 12 and 230 μmol m^{-2} s^{-1}. This estimate will aid future studies to determine the irradiance optimum of *Amphidinium gibbosum* strain Amp02.

Also interestingly, I observed a spike in cell abundance in all cultures on day 28, followed by a decline on day 32, with the cultures' densities increasing again through the end of the experiments, with final measurements on day 39. The decline on day 32 is caused by algal cell death, most likely due to starvation. While I do not know what lead to the subsequent recovery, there have been studies on this phenomenon in *E. coli*. Schink *et al.* reported that viable *E. coli* can feed on the carcasses of dead cells during starvation-induced cell death.[70] Amp02 algae cultures are not axenic but contain ciliate and multiple bacterial contaminations. When algal cells die, heterotrophic organisms in the culture might feed upon their carcasses, releasing inorganic waste products, which in turn may nourish the algae and support a return to growth. However, further studies are needed to determine the exact causes behind these dynamics.

4.2. Symbiosis establishment

In these experiments, I aimed to test whether and how symbiosis could be established in adult aposymbiotic *Waminoa* worms (and also juvenile worms) after exposure to either liquid cultures of Amp02 *Amphidinium* algae or symbiotic adult "donor" worms. I monitored not only symbiosis establishment as a factor of how many worms contained algae and the number of algae cells per infected worm but also the population size of worms in each experimental tank.

4.2.1. Asexual reproduction and population dynamics during algae exposure

Regarding the effects of algae exposure on worm asexual reproduction, I found that *Amphidinium* cells in the tanks at a concentration of 80 algal cells/mL did not affect the population size of adult *Waminoa* line C aposymbionts, as there was no significant

difference in population sizes of tanks exposed to Amp02 algae and the control tanks (no exposure).

In contrast, population sizes of aposymbionts exposed to symbiotic donors decreased during the first two weeks before increasing in week 3. The number of symbiotic donors, however, increased during all four weeks, suggesting a higher fitness of donors compared to aposymbionts in the tanks D1-D3. In addition to their high symbiont loads, I hypothesise that donors capture more food, primarily due to their larger bodies. I chose large donors and small aposymbionts to help distinguish them, which could have resulted in donors capturing more food and promoting aposymbiont mortality. The body sizes of donors and aposymbionts started to equalise after two weeks – one week before the number of aposymbionts in the tanks D1-D3 increased again, by which time nearly all of them had established symbiosis (Figure 5). Unfortunately, I cannot thoroughly compare the aposymbiont population dynamics in these tanks to the control tank D4, as it contained three small and one large aposymbiont. After body sizes had equalised, it was impossible to distinguish between the initially large and small individuals as they all had the same white body colour.

4.2.2. Establishment of stable symbioses from donors, not cultured algae

Exposure to cultured *A. gibbosum* strain Amp02 alone led to transient infection patterns, and thus failed to establish a stable symbiosis. Aposymbiotic and donor flatworms belong to *Waminoa sp.* line C, and Amp02 cultures were isolated from a different strain of *Waminoa* several years ago. Therefore, the symbiosis establishment may have failed due to incompatibility between symbiont and host strains.[51] So far, I have not used freshly isolated dinoflagellates from line C *Waminoa* because they have not survived in culture for more than a few weeks. Sandra Montaño Salazar is currently establishing a new isolation method based on florescence-activated cell sorting (FACS), which seems promising. If these isolation efforts are successful, to test if new isolates are efficient in infecting *Waminoa*, I suggest exposing aposymbionts to algae freshly isolated from the exact same host, line C *Waminoa*. Additionally, the duration of time the algae have been isolated and in culture could be a factor. Therefore, I would also suggest experiments testing exposure to freshly isolated algae versus algae isolated in the past weeks or months and kept in culture.

Furthermore, the number of algal cells added per week (80 cells/mL FASW) was likely

appropriate. *Waminoa* population sizes between the control and the algae-treated groups show no significant differences. However, future experiments could change the algae cell concentration to test whether higher concentrations might facilitate symbiosis establishment.

In contrast, I demonstrated that *Waminoa* line C flatworms can transfer their dinoflagellate endosymbionts to aposymbiotic individuals, resulting in a new stable association. My observations suggest that symbiotic donors provide some unknown factor allowing symbiosis to occur. To test whether successful infection depends on a host factor provided by living donors, aposymbionts should be exposed to donor animals and to macerated symbiotic *Waminoa* containing intact algal cells.

Along these lines of accompanying “host factor(s)” or compounds that facilitate uptake, it could be that the mode of dinoflagellate delivery impacts symbiosis establishment. Perhaps “naked” algae cells were not sufficiently detected and taken up by the worms. Therefore, to attempt to recapitulate the success of uptake from donor worms, future experiments could mix algae cultures and fresh isolates with *Artemia* and or *Tisbe* shrimp macerates, artificial mucus, or symbiotic *Waminoa* macerates after removing the original symbiont beforehand. As artificial mucus, I would suggest a low melting temperature 0.1% agarose gel, which could be supplemented with marine broth or specific compounds that might stimulate worm feeding and thus facilitate algae uptake.

Regarding compatibility between donor, recipient host, and algae strain for the experiments with juvenile aposymbiotic worms: *Waminoa* line W does not naturally host Amp02 algae, but another unidentified *Amphidinium* species, and therefore, the juvenile line W flatworms might not be able to symbiotically engage with Amp02 dinoflagellates, as reflected by the low infection rates. This incompatibility is further suggested by preliminary data generated by Cátia Pinto, showing successful infection of line W juveniles when exposed to adult line W but not line C donors. Moving forward, this experiment should be repeated with more juvenile tanks. Additionally, I would suggest exposing line W juveniles to symbionts freshly isolated from line W. So far, we cannot produce stable line W symbiont cultures. However, fresh isolates can survive in liquid cultures for a few weeks before their numbers diminish and could thus be used in experiments during this timeframe.

The long-term goal of these infection experiments is to identify which factors promote the

formation of stable associations, allowing us to establish endosymbiosis between chosen dinoflagellates and *Waminoa* flatworms. This would enable us to study specific dinoflagellates' effects on their host and how they change under different environmental conditions.

4.3. Identification of polyketides

Marine microorganisms are a rich source of bioactive natural products, and many of these compounds, including *Amphidinium* derived polyketides,[71-73] inhibit the growth of pathogens.[74] At the same time, sessile marine invertebrates frequently contain natural products and symbiotic microbes. Although marine defensive symbiosis is generally considered underexplored, some research suggest that invertebrate hosts gain a fitness advantage when exposed to predators or pathogens if they harbour symbionts or are presented with symbiont produced natural products. Lopanik proposed that the chemical defence provided by symbionts in marine invertebrates may be more common than currently believed.[44] Furthermore, naturally symbiotic *Amphidinium* dinoflagellates isolated from the Okinawan flatworm genus *Amphiscolops* and have been shown to produce polyketides in culture, supporting the possibility of polyketide production within symbiotic associations.[75-77] Based on these reports, Sandra Montaño Salazar and I hypothesised that *Amphidinium* dinoflagellates produce polyketides within their host.

We aimed to identify polyketides in symbiotic *Waminoa* line C flatworms and *Amphidinium gibbosum* strain Amp02 cultures by HPLC-MS/MS analysis. This experiment is the first step towards determining whether the dinoflagellate defends its worm host against pathogens and predators.

In collaboration with Prof. Wolfgang Wanek and Rahul Samrat from the Division of Terrestrial Ecosystem Research (TER) in CeMESS, University of Vienna, we first implemented a generic lipid extraction protocol to concentrate putative polyketides. However, the HPLC-MS/MS showed that MS1 peaks with masses potentially corresponding to polyketides had very low intensities, which could represent background noise. Additionally, we encountered technical issues since the machines needed repair, and the resulting time delay exceeded the limits of this thesis.

Hence, we shifted our approach, implementing a methanol-based extraction method and analysing samples by HRES-HPLC-MS/MS. Here, we reported preliminary results primarily based on MS1 data. This data does not fully confirm the presence of polyketides

but it is the first step towards developing a robust pipeline.

Salt reduction is the first step of sample preparation and a critical step in preparing these marine samples for measurement with the salt-sensitive HPLC MS/MS instrument. For *Waminoa* flatworm samples, we developed and recommended Salt Reduction Protocol B as it reduces the exposure to low osmotic pressure and leaves the worms intact.

Following salt reduction, we freeze-dried the samples and extracted them according to an adjusted methanol-based protocol for amphidinols developed and published by Wellkamp *et al.*[46] According to the cLogP predictions with ChemDraw[48], several polyketides should be soluble in methanol, while others should prefer more polar or apolar solvents. In future experiments, we will test other extraction procedures like the Bligh-Dyer method, which has a polar phase consisting of methanol and water and an apolar chloroform phase.[78] Analysing the different phases could improve the detection of compounds with low methanol solubility.

The methanolic extracts were analysed with HRES-HPLC-MS/MS in collaboration with Valentin Göldner from the University of Vienna. According to the recommendation of Steckel *et al.,* the negative ionisation mode (ES-) is better suited for molecules with acidic characteristics, as deprotonation is more favourable than protonation.[56] As the polyketide of interest does possess weak acidic properties, we chose negative ionisation. Nonetheless, the current methodology most likely limits the detection efficiency. The overall pKa values and the functional groups of the polyketides of interest point towards low deprotonation tendencies. Some polyketides carry carboxylic or sulfonic acid groups, which, are much more likely to lose a proton. However, most of the compounds only possess ketonic and alcoholic functional groups, which are generally difficult to ionise.[56] Many studies that identified polyketides used a positive ionisation mode (ES+) but did not explain the reasons behind this choice.[75,79,80] Nuzzo *et al.* chose ES+ mode to identify amphidinol 18 and 19, despite amphidinol 19 having a sulfonic acid functional group, which is easily detectable with negative not positive ionisation.[79,81] However, they, like others, worked with purified compounds, making the detection even at low ionisation efficiency easier, and supplemented their analysis with NMR and other techniques.[75,79,80] Since we worked with a mixture of many extracted compounds, we had to find different solutions to increase the detectability of polyketides. Moving forward, we will implement derivatisation to increase ionisation. Hydroxylamine was previously used to form oximes with ketones, significantly increasing ionisation efficiency. Anhydrides like 2-

sulfobenzonic anhydride are suitable derivatisation agents for aliphatic alcohols to improve detection in ES- mode.[82]

Another limitation is the lack of reference MS2 spectra. During tandem mass spectrometry, the exact masses and retention times of compounds in the sample are measured, followed by the fragmentation of compounds. The resulting fragmentation patterns are highly specific to the parent molecule. While the physicochemical and structural properties of the detection targets are important, only subsequent comparisons between measured and reported fragmentation patterns allow definite identification.[83] Therefore, it is unfortunate that we could not find such fragmentation patterns for these compounds in the literature.

Alternatively, MS2 spectra of isolated compounds can be generated and compared to the unknown masses detected in mixed extracts. However, polyketides are seldomly commercially available, and we could find no commercial or other sources of these *Amphidinium* polyketides. Therefore, we chose dinophysistoxin-1 (DTX-1) as a standard. DTX-1, produced by marine dinoflagellates such as *Dinophysis*, and other okadaic acid analogs are causative agents of shellfish poisoning.[84,85] DTX-1 is biosynthesised through the condensation of ketogenic fragments, three of which are classical polyketides.[86] Although dinophysistoxin-1 is not the preferred standard, it is sufficiently similar to polyketides to serve as a provisional standard. In the future, we will intensify our search for standards of polyketides produced by *Amphidinium* species to develop a library of their fragmentation patterns for identification purposes.

5. Conclusion

The primary objectives of this thesis were to enhance our understanding of *Amphidinium* dinoflagellates, specifically their characteristics in free-living liquid culture, reflecting harmful algal blooms (HABs), and in photosymbiosis. To that end, I explored their growth dynamics under varying light conditions, investigated if symbiosis establishment can be controlled, and aimed to identify polyketides in symbiotic flatworms and cultured algae.

This research has shown that high light intensity (HLI) compared to low light intensity (LLI) increased the growth rate of Amp02 dinoflagellates during the first week of exposure, but led to bleaching from day 32 until day 39, the end of the experiment. These findings suggest that the optimal irradiance level lies between photon flux densities of 12 to 230 μmol m^{-2} s^{-1}. Future research should focus on algal growth at specific photon flux densities to refine this estimate.

The observed decline in cell density in all algal cultures on day 32 is most likely caused by starvation-induced cell death. The subsequent rise in algal cell concentration points towards releasing inorganic nutrients by dying algal and, since the cultures carry contaminations, bacterial cells. This observation should be explored further to gain a more comprehensive understanding of how microbial communities affect algal growth dynamics and HABs.

Moreover, the research into symbiosis establishment with *Waminoa* flatworms provided insights into the complexities of symbiotic relationships. The findings suggest that a host-derived factor is needed for successful symbiosis establishment, as adult aposymbiotic *Waminoa* line C worms became symbiotic when exposed to donors but not to cultured algae alone. The unsuccessful infection of aposymbiotic adult and juvenile flatworms with cultured algae might be due to symbiotic incompatibility, as they do not naturally host this exact strain (Amp02) of *Amphidinium*. Future experiments should aim to identify the potential host factor, and test infections with compatible *Amphidinium* strains, which are currently being isolated by Sandra Montaño Salazar. These explorations will help continue to establish *Waminoa* and *Amphidinium* as a model system for studying non-cnidarian marine photosymbiosis, which is crucial for assessing the impact of environmental changes on these relationships.

Besides nutrient exchange, many aspects of marine photosymbioses remain elusive, particularly the possibility of a defensive symbiosis for the host, facilitated by symbiont-produced compounds. This thesis aimed to identify polyketides in symbiotic flatworms and cultured dinoflagellates. The limitations of the current methodologies, such as the low ionisability of many polyketides, were recognised and will be addressed in future experiments. Moving forward, more extracts will be analysed, including samples of aposymbiotic flatworms. The analysis will be expanded by the use of predictive models as reported by Gorynski *et al.*[61] As these models do not replace comparison to fragmentation patterns of isolated compounds, our group aims to gain access to polyketide isolates.

Future research should prioritise generating axenic cultures, identifying the putative host factor for symbiosis establishment, and refining methods for polyketide detection in marine organisms. These efforts will enhance our understanding of marine photosymbioses and their ecological role, ultimately contributing to strategies aimed at preserving marine ecosystems in the face of climate change and other anthropogenic stressors.

6. References

1 De Bary, A. *Die erscheinung der symbiose: Vortrag gehalten auf der versammlung deutscher naturforscher und aerzte zu cassel*. (Trübner, 1879).

2 Rosenberg, E., Sharon, G. & Zilber-Rosenberg, I. The hologenome theory of evolution contains Lamarckian aspects within a Darwinian framework. *Environmental microbiology* **11**, 2959-2962 (2009).

3 Archibald, J. M. in *Advances in botanical research* Vol. 64 87-118 (Elsevier, 2012).

4 Johnson, M. D. The acquisition of phototrophy: adaptive strategies of hosting endosymbionts and organelles. *Photosynthesis research* **107**, 117-132 (2011).

5 Yellowlees, D., Rees, T. A. V. & Leggat, W. Metabolic interactions between algal symbionts and invertebrate hosts. *Plant, cell & environment* **31**, 679-694 (2008).

6 Falkowski, P. G., Dubinsky, Z., Muscatine, L. & McCloskey, L. Population control in symbiotic corals. *Bioscience* **43**, 606-611 (1993).

7 Muscatine, L. & Hand, C. Direct evidence for the transfer of materials from symbiotic algae to the tissues of a coelenterate. *Proceedings of the National Academy of Sciences* **44**, 1259-1263 (1958).

8 Burriesci, M. S., Raab, T. K. & Pringle, J. R. Evidence that glucose is the major transferred metabolite in dinoflagellate–cnidarian symbiosis. *Journal of Experimental Biology* **215**, 3467-3477 (2012).

9 Lipps, J. H. & Stanley, G. D. Photosymbiosis in past and present reefs. *Coral Reefs at the Crossroads*, 47-68 (2016).

10 Not, F. *et al.* Photosymbiosis in marine pelagic environments. *The Marine Microbiome: An Untapped Source of Biodiversity and Biotechnological Potential*, 305-332 (2016).

11 Kleindorfer, S. & Mitchell, J. G. Biological networks: rainforests, coral reefs, and the Galapagos Islands. *Network challenge: the strategy, profit, and risk in an interlinked world. Pennsylvania, US: Wharton School Publishing*, 85-104 (2009).

12 Darwin, C. *The structure and distribution of coral reefs*. Vol. 15 (D. Appleton, 1889).

13 Cui, G. *et al.* Molecular insights into the Darwin paradox of coral reefs from the sea anemone Aiptasia. *Science Advances* **9**, eadf7108 (2023).

14 Souter, D. *et al.* (Global Coral Reef Monitoring network (GCRMN) and International Coral Reef …, 2021).

15 Trench, R. Microalgal-invertebrate Ssmbioses-a review. *Endocyt. Cell. Res.* **9**, 135-175 (1993).

16 Kunihiro, S. & Reimer, J. D. Phylogenetic analyses of Symbiodinium isolated from Waminoa and their anthozoan hosts in the Ryukyu Archipelago, southern Japan.

Symbiosis **76**, 253-264 (2018).

17 Granéli, E. & Turner, J. T. in *Ecology of Harmful Algae* (eds Edna Granéli & Jefferson T. Turner) 3-7 (Springer Berlin Heidelberg, 2006).

18 Danielsdottir, M. G., Brett, M. T. & Arhonditsis, G. B. Phytoplankton food quality control of planktonic food web processes. *Hydrobiologia* **589**, 29-41 (2007).

19 Schleyer, G. & Vardi, A. Algal blooms. *Current Biology* **30**, R1116-R1118 (2020).

20 Gobler, C. J. *et al.* Ocean warming since 1982 has expanded the niche of toxic algal blooms in the North Atlantic and North Pacific oceans. *Proceedings of the National Academy of Sciences* **114**, 4975-4980 (2017).

21 Karlson, B. *et al.* Harmful algal blooms and their effects in coastal seas of Northern Europe. *Harmful Algae* **102**, 101989 (2021).

22 Summers, E. J. & Ryder, J. L. A critical review of operational strategies for the management of harmful algal blooms (HABs) in inland reservoirs. *Journal of Environmental Management* **330**, 117141 (2023).

23 Mitrovic, S. M., Hardwick, L. & Dorani, F. Use of flow management to mitigate cyanobacterial blooms in the Lower Darling River, Australia. *Journal of Plankton Research* **33**, 229-241 (2011).

24 Kobayashi, J. i. & Kubota, T. Bioactive macrolides and polyketides from marine dinoflagellates of the genus Amphidinium. *Journal of natural products* **70**, 451-460 (2007).

25 Barone, M. E. *et al.* Antibacterial activity and amphidinol profiling of the marine dinoflagellate Amphidinium carterae (Subclade III). *International Journal of Molecular Sciences* **22**, 12196 (2021).

26 Murray, S. A. *et al.* A fish kill associated with a bloom of Amphidinium carterae in a coastal lagoon in Sydney, Australia. *Harmful Algae* **49**, 19-28 (2015).

27 Al-Qasmi, M., Raut, N., Talebi, S., Al-Rajhi, S. & Al-Barwani, T. in *Proceedings of the world congress on engineering.* 1-7.

28 Chen, X.-C. *et al.* Reducing harmful algae in raw water by light-shading. *Process Biochemistry* **44**, 357-360 (2009).

29 Karafas, S., Teng, S. T., Leaw, C. P. & Alves-de-Souza, C. An evaluation of the genus Amphidinium (Dinophyceae) combining evidence from morphology, phylogenetics, and toxin production, with the introduction of six novel species. *Harmful Algae* **68**, 128-151 (2017).

30 Tyler, S., Artois, T.; Schilling, S.; Hooge, M.; Bush, L.F. World List of turbellarian worms: Acoelomorpha, Catenulida, Rhabditophora. Acoela. (2006-2024).

31 Rola, M. *et al.* Cladobranchia (Gastropoda, Nudibranchia) as a promising model to understand the molecular evolution of photosymbiosis in animals. *Frontiers in Marine Science* **8**, 745644 (2022).

32 Bien, T., Hambleton, E. A., Dreisewerd, K. & Soltwisch, J. Molecular insights into symbiosis—mapping sterols in a marine flatworm-algae-system using high spatial resolution MALDI-2-MS imaging with ion mobility separation. *Analytical and Bioanalytical Chemistry* **413**, 2767-2777 (2021).

33 Davy, S. K., Allemand, D. & Weis, V. M. Cell biology of cnidarian-dinoflagellate symbiosis. *Microbiology and Molecular Biology Reviews* **76**, 229-261 (2012).

34 Jacobovitz, M. R., Hambleton, E. A. & Guse, A. Unlocking the complex cell biology of coral–dinoflagellate symbiosis: A model systems approach. *Annual Review of Genetics* **57**, 411-434 (2023).

35 Achatz, J. G., Chiodin, M., Salvenmoser, W., Tyler, S. & Martinez, P. The Acoela: on their kind and kinships, especially with nemertodermatids and xenoturbellids (Bilateria incertae sedis). *Organisms Diversity & Evolution* **13**, 267-286 (2013).

36 Kunihiro, S. *et al.* Morphological and phylogenetic diversity of Waminoa and similar flatworms (Acoelomorpha) in the western Pacific Ocean. *Zoology* **136**, 125692 (2019).

37 Ogunlana, M. V. *et al.* Waminoa brickneri n. sp.(Acoela: Acoelomorpha) associated with corals in the Red Sea. *Zootaxa* **1008**, 1–11-11–11 (2005).

38 Winsor, L. Marine Turbellaria (Acoela) from north Queensland. *Memoirs of the Queensland Museum* **28**, 785--800 (1990).

39 Barneah, O., Brickner, I., Hooge, M., Weis, V. M. & Benayahu, Y. First evidence of maternal transmission of algal endosymbionts at an oocyte stage in a triploblastic host, with observations on reproduction in Waminoa brickneri (Acoelomorpha). *Invertebrate Biology* **126**, 113-119 (2007).

40 Hikosaka-Katayama, T., Koike, K., Yamashita, H., Hikosaka, A. & Koike, K. Mechanisms of maternal inheritance of dinoflagellate symbionts in the acoelomorph worm Waminoa litus. *Zoological science* **29**, 559-567 (2012).

41 Kwan, J. C. *et al.* Genome streamlining and chemical defense in a coral reef symbiosis. *Proceedings of the National Academy of Sciences* **109**, 20655-20660 (2012).

42 Flórez, L. V., Biedermann, P. H. W., Engl, T. & Kaltenpoth, M. Defensive symbioses of animals with prokaryotic and eukaryotic microorganisms. *Nat Prod Rep* **32**, 936 (2015).

43 Mydlarz, L. D., Jacobs, R. S., Boehnlein, J. & Kerr, R. G. Pseudopterosin biosynthesis in Symbiodinium sp., the dinoflagellate symbiont of Pseudopterogorgia elisabethae. *Chemistry & biology* **10**, 1051-1056 (2003).

44 Lopanik, N. B. Chemical defensive symbioses in the marine environment. *Functional Ecology* **28**, 328-340 (2014).

45 Maegele, I. *et al.* A predatory gastrula leads to symbiosis-independent settlement in Aiptasia. *Proceedings of the National Academy of Sciences* **120**, e2311872120

(2023).

46 Wellkamp, M. *et al.* LC-MS/MS method development for the discovery and identification of amphidinols produced by Amphidinium. *Marine drugs* **18**, 497 (2020).

47 Schmid, R. *et al.* Integrative analysis of multimodal mass spectrometry data in MZmine 3. *Nature biotechnology* **41**, 447-449 (2023).

48 Informatics, P.

49 Xialin Pan, H. W., Cuiyu Li, John Z. H. Zhang, Changge Ji. Vol. 61 (Journal of Chemical Information and Modeling, 2021).

50 Bucher, M., Wolfowicz, I., Voss, P. A., Hambleton, E. A. & Guse, A. Development and symbiosis establishment in the cnidarian endosymbiosis model Aiptasia sp. *Scientific reports* **6**, 19867 (2016).

51 Hambleton, E. A., Guse, A. & Pringle, J. R. Similar specificities of symbiont uptake by adults and larvae in an anemone model system for coral biology. *Journal of Experimental Biology* **217**, 1613-1619 (2014).

52 BioRender.com. (2024).

53 Kim S, C. J., Cheng T, Gindulyte, A., He, J., He, S., Li, Q., Shoemaker, B. A., Thiessen, P. A., Yu, B., Zaslavsky, L., Zhang, J., & Bolton, E. E. PubChem 2023 update. *Nucleic Acids Res* **51** (2023).

54 *ChemSpider Home Page*, <http://www.chemspider.com/ >

55 *J-Global Homepage* <https://jglobal.jst.go.jp/en>

56 Steckel, A. & Schlosser, G. An organic chemist's guide to electrospray mass spectrometric structure elucidation. *Molecules* **24**, 611 (2019).

57 Constantopoulos, T. L., Jackson, G. S. & Enke, C. G. Effects of salt concentration on analyte response using electrospray ionization mass spectrometry. *Journal of the American Society for Mass Spectrometry* **10**, 625-634 (1999).

58 Pinho, S. P. & Macedo, E. A. Representation of salt solubility in mixed solvents: A comparison of thermodynamic models. *Fluid Phase Equilibria* **116**, 209-216 (1996).

59 Box, K. & Comer, J. Using measured pKa, LogP and solubility to investigate supersaturation and predict BCS class. *Current drug metabolism* **9**, 869-878 (2008).

60 Scientific, T. F. *Calculate reagent log P values to determine solubility characteristics.*, <Retrieved from: https://assets.thermofisher.com/TFS-Assets/LSG/Application-Notes/TR0056-Calc-logP.pdf> (n.d.).

61 Goryński, K. *et al.* Quantitative structure–retention relationships models for prediction of high performance liquid chromatography retention time of small molecules: endogenous metabolites and banned compounds. *Analytica chimica*

acta **797**, 13-19 (2013).

62 Böcker, S., Letzel, M. C., Lipták, Z. & Pervukhin, A. SIRIUS: decomposing isotope patterns for metabolite identification. *Bioinformatics* **25**, 218-224 (2009).

63 Möller, K. *et al.* Effects of bottom-up factors on growth and toxin content of a harmful algae bloom dinoflagellate. *Limnology and Oceanography* **69**, 1335-1349 (2024).

64 Dou, M., Ma, X., Zhang, Y., Zhang, Y. & Shi, Y. Modeling the interaction of light and nutrients as factors driving lake eutrophication. *Ecological Modelling* **400**, 41-52 (2019).

65 Edwards, K. F., Thomas, M. K., Klausmeier, C. A. & Litchman, E. Light and growth in marine phytoplankton: allometric, taxonomic, and environmental variation. *Limnology and Oceanography* **60**, 540-552 (2015).

66 Chan, A. T. COMPARATIVE PHYSIOLOGICAL STUDY OF MARINE DIATOMS AND DINOFLAGELLATES IN RELATION TO IRRADIANCE AND CELL SIZE. I. GROWTH UNDER CONTINUOUS LIGHT 1, 2. *Journal of Phycology* **14**, 396-402 (1978).

67 Lesser, M. P. Elevated temperatures and ultraviolet radiation cause oxidative stress and inhibit photosynthesis in ymbiotic dinoflagellates. *Limnology and oceanography* **41**, 271-283 (1996).

68 Rodríguez, J. G. *et al.* Culture of dinoflagellates in a fed-batch and continuous stirred-tank photobioreactors: Growth, oxidative stress and toxin production. *Process Biochemistry* **45**, 660-666 (2010).

69 Wise, R. R. & Naylor, A. W. Chilling-enhanced photooxidation: evidence for the role of singlet oxygen and superoxide in the breakdown of pigments and endogenous antioxidants. *Plant Physiology* **83**, 278-282 (1987).

70 Schink, S. J., Biselli, E., Ammar, C. & Gerland, U. Death rate of E. coli during starvation is set by maintenance cost and biomass recycling. *Cell systems* **9**, 64-73. e63 (2019).

71 Cutignano, A., Nuzzo, G., Sardo, A. & Fontana, A. The missing piece in biosynthesis of amphidinols: First evidence of glycolate as a starter unit in new polyketides from Amphidinium carterae. *Marine drugs* **15**, 157 (2017).

72 Echigoya, R., Rhodes, L., Oshima, Y. & Satake, M. The structures of five new antifungal and hemolytic amphidinol analogs from Amphidinium carterae collected in New Zealand. *Harmful Algae* **4**, 383-389 (2005).

73 Kubota, T. *et al.* Amphidinin G, a putative biosynthetic precursor of amphidinin A from marine dinoflagellate Amphidinium sp. *Tetrahedron letters* **56**, 990-993 (2015).

74 Carroll, A. R., Copp, B. R., Grkovic, T., Keyzers, R. A. & Prinsep, M. R. Marine natural products. *Natural Product Reports* **41**, 162-207 (2024).

75 Kobayashi, J. i., Yamaguchi, N. & Ishibashi, M. Amphidinolide M, a novel 29-membered macrolide from the cultured marine dinoflagellate Amphidinium sp. *The Journal of Organic Chemistry* **59**, 4698-4700 (1994).

76 Kobayashi, J. i. *et al.* Amphidinolide-A, a novel antineoplastic macrolide from the marine dinoflagellate Amphidinium sp. *Tetrahedron letters* **27**, 5755-5758 (1986).

77 Kobayashi, J., Sato, M. & Ishibashi, M. Amphidinolide J: A cytotoxic macrolide from the marine dinoflagellate Amphidinium sp. Determination of the absolute stereochemistry. *The Journal of Organic Chemistry* **58**, 2645-2646 (1993).

78 Bligh, E. G. & Dyer, W. J. A rapid method of total lipid extraction and purification. *Canadian journal of biochemistry and physiology* **37**, 911-917 (1959).

79 Nuzzo, G., Cutignano, A., Sardo, A. & Fontana, A. Antifungal amphidinol 18 and its 7-sulfate derivative from the marine dinoflagellate Amphidinium carterae. *Journal of natural products* **77**, 1524-1527 (2014).

80 Ishibashi, M., Sato, M. & Kobayashi, J. Amphidinolide K, a new 19-membered macrolide from the cultured symbiotic dinoflagellate Amphidinium sp. *The Journal of Organic Chemistry* **58**, 6928-6929 (1993).

81 Socher, G., Nussbaum, R., Rissler, K. & Lankmayr, E. Analysis of sulfonated compounds by ion-exchange high-performance liquid chromatography–mass spectrometry. *Journal of Chromatography A* **912**, 53-60 (2001).

82 Qi, B.-L. *et al.* Derivatization for liquid chromatography-mass spectrometry. *TrAC Trends in Analytical Chemistry* **59**, 121-132 (2014).

83 Brown, M. *et al.* Mass spectrometry tools and metabolite-specific databases for molecular identification in metabolomics. *Analyst* **134**, 1322-1332 (2009).

84 安元健 *et al.* Identification of Dinophysis fortii as the causative organism of diarrhetic shellfish poisoning. *日本水産学会誌* **46**, 1405-1411 (1980).

85 Suzuki, T. & Mitsuya, T. Comparison of dinophysistoxin-1 and esterified dinophysistoxin-1 (dinophysistoxin-3) contents in the scallop Patinopecten yessoensis and the mussel Mytilus galloprovincialis. *Toxicon* **39**, 905-908 (2001).

86 Norte, M., Padilla, A. & Fernández, J. J. Studies on the biosynthesis of the polyether marine toxin dinophysistoxin-1 (DTX-1). *Tetrahedron letters* **35**, 1441-1444 (1994).

7. Appendix

Table 9: 100 literature-reported polyketides produced by *Amphidinium* species with database entries in PubChem, ChemSpider, or Jglobal. The cLogP and pKa values are theoretical predictions.

Polyketide	Formula	cLogP	pKa
Amdigenol E	$C_{82}H_{137}NaO_{37}S$	-13.9134	12.2475862
Amdigenol G	$C_{60}H_{101}NaO_{25}S$	-5.64919	12.5089474
Amphezonol A	$C_{62}H_{114}O_{24}$	-8.70259	12.5285714
Amphidinin A	$C_{22}H_{38}O_4$	3.4738	13.75
Amphidinin B	$C_{25}H_{42}O_7$	4.9886	4.34
Amphidinin G	$C_{22}H_{38}O_4$	2.9068	13.7225
Amphidinoketide I	$C_{24}H_{38}O_4$	5.1874	NA
Amphidinoketide II	$C_{24}H_{38}O_4$	5.2764	NA
Amphidinol 10	$C_{66}H_{112}O_{23}$	-5.14119	12.7161905
Amphidinol 11	$C_{71}H_{122}O_{28}S$	-5.39365	12.7185714
Amphidinol 12	$C_{68}H_{115}NaO_{26}S$	-4.37155	12.6505
Amphidinol 13	$C_{70}H_{117}NaO_{26}S$	-3.93435	12.6655
Amphidinol 14	$C_{59}H_{101}NaO_{25}S$	-5.14175	12.6115789
Amphidinol 15	$C_{59}H_{102}O_{22}$	-5.01959	12.6805
Amphidinol 17	$C_{63}H_{110}O_{24}S$	-2.6822	11.7926316
Amphidinol 18	$C_{71}H_{122}O_{24}$	-3.05479	12.7404762
Amphidinol 19	$C_{71}H_{122}NaO_{27}S^+$	-3.11479	11.8947619
Amphidinol 2	$C_{71}H_{122}O_{25}$	-4.99849	12.7890909

Amphidinol 20	$C_{87}H_{152}O_{27}$	-3.75419	12.8748
Amphidinol 21	$C_{94}H_{166}O_{30}$	-5.94938	12.9182143
Amphidinol 22	$C_{84}H_{140}O_{31}$	-7.22859	12.6669231
Amphidinol 24	$C_{66}H_{116}O_{27}$	-10.9959	12.624
Amphidinol 3	$C_{70}H_{118}O_{23}$	-3.34239	12.7280952
Amphidinol 4	$C_{68}H_{116}O_{23}$	-3.97639	12.7280952
Amphidinol 5	$C_{72}H_{122}O_{24}$	-3.45139	12.1618182
Amphidinol 6	$C_{70}H_{120}O_{24}$	-4.08539	12.1618182
Amphidinol 7	$C_{59}H_{99}NaO_{23}S$	-2.24009	12.6182353
Amphidinol 9	$C_{70}H_{118}O_{23}$	-3.53919	12.7461905
Amphidinol A	$C_{69}H_{126}O_{24}$	-2.3268	12.7409524
Amphidinol B	$C_{69}H_{126}O_{27}S$	-2.38679	11.8952381
Amphidinolactone A	$C_{69}H_{124}O_{23}$	2.9079	13.215
Amphidinolactone B	$C_{20}H_{30}O_4$	3.3027	12.7225
Amphidinolide A	$C_{32}H_{54}O_8$	4.7236	13.195
Amphidinolide B	$C_{31}H_{46}O_7$	4.2526	12.895
Amphidinolide B1	$C_{32}H_{50}O_8$	4.2526	12.895
Amphidinolide B2	$C_{32}H_{50}O_8$	4.2526	12.895
Amphidinolide B3	$C_{32}H_{50}O_8$	4.2526	12.895
Amphidinolide B4	$C_{32}H_{50}O_8$	5.4836	12.94
Amphidinolide B5	$C_{32}H_{50}O_7$	5.4836	12.94

Amphidinolide B6	$C_{32}H_{50}O_7$	4.4715	12.91
Amphidinolide B7	$C_{32}H_{54}O_8$	5.4836	12.94
Amphidinolide C	$C_{32}H_{50}O_7$	3.8414	12.9075
Amphidinolide C2	$C_{41}H_{62}O_{10}$	4.7874	13.0266667
Amphidinolide D	$C_{43}H_{64}O_{11}$	4.2526	12.895
Amphidinolide E	$C_{32}H_{50}O_8$	4.5614	13.07
Amphidinolide F	$C_{30}H_{44}O_6$	3.0884	13.13
Amphidinolide G	$C_{35}H_{52}O_9$	4.2209	12.9325
Amphidinolide G2	$C_{32}H_{50}O_8$	4.2209	12.9325
Amphidinolide G3	$C_{32}H_{50}O_8$	3.5049	12.9325
Amphidinolide H	$C_{32}H_{52}O_8$	4.2809	12.85
Amphidinolide H2	$C_{32}H_{50}O_8$	4.2809	12.85
Amphidinolide H3	$C_{32}H_{50}O_8$	4.2809	12.85
Amphidinolide H4	$C_{32}H_{50}O_8$	4.5649	12.85
Amphidinolide H5	$C_{32}H_{52}O_8$	4.5649	12.85
Amphidinolide J	$C_{32}H_{52}O_8$	5.1239	13.275
Amphidinolide K	$C_{24}H_{38}O_4$	5.0877	13.82
Amphidinolide L	$C_{27}H_{40}O_5$	5.0938	11.5075
Amphidinolide M	$C_{32}H_{50}O_8$	4.1728	13.7025
Amphidinolide N	$C_{43}H_{66}O_9$	-0.209301	11.6957143
Amphidinolide O	$C_{33}H_{54}O_{12}$	0.714749	11.94

Amphidinolide P	$C_{21}H_{28}O_6$	2.67125	12
Amphidinolide Q	$C_{22}H_{30}O_5$	3.9764	12.48
Amphidinolide R	$C_{21}H_{34}O_4$	4.9739	13.56
Amphidinolide S	$C_{24}H_{38}O_4$	4.8619	12.94
Amphidinolide T1	$C_{24}H_{36}O_4$	4.9281	12.89
Amphidinolide T2	$C_{25}H_{42}O_5$	2.7116	13.13
Amphidinolide T3	$C_{26}H_{44}O_6$	4.3896	12.96
Amphidinolide T4	$C_{25}H_{42}O_5$	4.3896	12.96
Amphidinolide T5	$C_{25}H_{42}O_5$	4.3896	12.96
Amphidinolide U	$C_{25}H_{42}O_5$	4.5829	13.3
Amphidinolide V	$C_{34}H_{50}O_7$	4.2267	13.63
Amphidinolide W	$C_{25}H_{32}O_4$	4.7359	13.6
Amphidinolide X	$C_{24}H_{38}O_4$	4.2459	NA
Amphidinolide Y	$C_{26}H_{40}O_6$	3.4856	13.08
Amphirionin-2	$C_{26}H_{42}O_6$	5.4615	13.97
Amphirionin-4	$C_{32}H_{50}O_5$	5.5257	13.81
Amphirionin-5	$C_{26}H_{40}O_3$	4.3088	13.725
Carteraol E	$C_{32}H_{54}O_7$	-1.57009	12.6910526
Colopsinol A	$C_{74}H_{126}O_{24}$	4.37147	12.4766667
Colopsinol B	$C_{71}H_{120}O_{25}S$	3.28217	12.5838462
Colopsinol C	$C_{68}H_{113}NaO_{25}S$	5.51471	12.905

Colopsinol D	$C_{62}H_{103}NaO_{20}S$	6.2994	10.9263636
Colopsinol E	$C_{71}H_{118}O_{24}S$	6.60401	12.8011111
Dinophysistoxin 1	$C_{65}H_{109}NaO_{20}S$	2.9273	10.406
Iriomoteolide 10a	$C_{35}H_{60}O_7$	5.9093	13.775
Iriomoteolide 12a	$C_{25}H_{40}O_5$	3.6234	12.47
Iriomoteolide 1a	$C_{29}H_{46}O_7$	2.72455	12.05
Iriomoteolide 1b	$C_{29}H_{46}O_7$	2.3108	12.24
Iriomoteolide 1c	$C_{30}H_{48}O_7$	3.25355	12.0625
Iriomoteolide 3a	$C_{25}H_{38}O_6$	2.1247	13.41
Karatungiol A	$C_{74}H_{134}O_{29}$	-5.38109	12.3657692
Karatungiol B	$C_{74}H_{132}O_{28}$	-4.45189	12.3528
Lingshuiol	$C_{69}H_{122}O_{25}$	-3.08119	12.46
Lingshuiol A	$C_{66}H_{112}O_{20}$	1.1898	12.6133333
Lingshuiol B	$C_{60}H_{99}NaO_{23}S$	-2.51819	12.54
Luteophanol A	$C_{60}H_{102}O_{25}S$	-5.80419	11.7495
Luteophanol B	$C_{67}H_{116}O_{25}$	-7.60939	12.6330435
Luteophanol C	$C_{67}H_{116}O_{25}$	-7.08039	12.633913
Luteophanol D	$C_{67}H_{116}O_{25}$	-7.80939	12.6482609
Symbiopolyol	$C_{60}H_{99}NaO_{23}S$	-2.51819	12.54

Table 10: List of all MS1 peaks with a mass matching a polyketide detected by HRES-HPLC-MS/MS. "/" in the names of annotated polyketides indicates several compounds with the same exact mass and chemical formula. "Adduct" indicates to which kind of adduct of the polyketide the mass corresponds. "Score" refers to the annotation score, which is a measure of confidence in MZmine that takes multiple spectral features into account. Retention time ("rt", given in minutes) is the time between the sample's injection and the detection of the mass. "Area" refers to the area enclosed under the peak and is crucial for quantification analyses. "mz" is the mass-to-charge ratio. "Samples" indicate, in which samples of the organisms the mass was detected. Samples AR1, AR2: *Artemia salina* shrimp as worm food; samples A2, A3: *Amphidinium gibbosum* algae strain Amp02 in liquid culture; samples SW3, SW4: symbiotic adults of *Waminoa* line C flatworms (see Table 3 for detailed organism and sample information)

Polyketide	Adduct	Score	rt	area	mz	Samples
Amphidinin A	[M-H]-	0.973	12.0631	7.65E+04	365.26968	AR1, AR2, A2, A3, SW3
Amphidinin A	[M-H]-	0.942	12.3238	1.27E+05	365.26963	A2, A3, SW3, SW4
Amphidinolactone A	[M-H]-	0.906	7.9794	2.92E+04	333.20729	AR1, AR2, A2
Amphidinolactone A	[M-H]-	0.949	8.1273	1.10E+04	333.20722	AR1, AR2, A2
Amphidinolactone A	[M-H]-	0.853	8.2357	1.16E+04	333.20738	AR1, AR2, A2
Amphidinolactone A	[M-H]-	0.94	8.3067	2.60E+04	333.20723	AR1, AR2
Amphidinolactone A	[2M-H]-	0.295	15.0097	3.12E+04	667.4239	AR1
Amphidinolactone A	[2M-H]-	0.776	16.176	1.82E+05	667.4208	A2, A3
Amphidinolide A	[M-H]-	0.976	9.1801	5.20E+04	529.31701	SW3, SW4
Amphidinolide A	[M-H]-	0.765	10.2063	3.72E+04	529.31646	SW3, SW4
Amphidinolide A	[M-H]-	0.917	10.9847	9.69E+04	529.31686	SW3, SW4

Amphidinolide A	[M-H]-	0.94	11.5151	4.88E+05	529.31692	SW3, SW4
Amphidinolide B/B1/D	[M-H]-	0.85	6.1708	4.66E+05	561.34287	SW3, SW4
Amphidinolide B/B1/D	[M-H]-	0.763	7.0094	1.91E+05	561.34263	SW3, SW4
Amphidinolide B/B1/D	[M-H]-	0.849	7.1376	1.01E+06	561.34287	SW3, SW4
Amphidinolide B/B1/D	[M-H]-	0.819	8.0511	6.72E+05	561.34279	SW3, SW4
Amphidinolide B/B1/D	[M-H]-	0.886	8.2563	4.30E+05	561.34297	SW3, SW4
Amphidinolide B/B1/D	[M-H]-	1	9.6758	5.92E+05	561.34329	SW3, SW4
Amphidinolide B/B1/D	[M-H]-	0.983	10.1724	6.55E+05	561.34325	SW3, SW4
Amphidinolide B/B1/D	[M-H]-	0.954	10.5998	2.62E+06	561.34316	SW3, SW4
Amphidinolide B4/B5/B7	[M-H]-	0.86	7.9153	7.74E+05	545.348	SW3, SW4
Amphidinolide B4/B5/B7	[M-H]-	0.925	9.0095	6.11E+05	545.34817	SW3, SW4
Amphidinolide B4/B5/B7	[M-H]-	0.896	9.0773	1.49E+06	545.34809	SW3, SW4
Amphidinolide B4/B5/B7	[M-H]-	0.865	9.6244	8.59E+04	545.34801	SW3, SW4

Amphidinolide B4/B5/B7	[M-H]-	0.972	10.0614	2.91E+05	545.3483	SW3, SW4
Amphidinolide B4/B5/B7	[M-H]-	0.878	11.2332	2.24E+05	545.34871	SW3, SW4
Amphidinolide B4/B5/B7	[M-H]-	0.984	11.9175	2.07E+06	545.34834	SW3, SW4
Amphidinolide B4/B5/B7	[M-H]-	0.992	12.5481	1.63E+06	545.34836	SW3, SW4
Amphidinolide C	[M-H]-	0.929	12.4198	3.86E+04	713.42728	SW3, SW4
Amphidinolide C	[M-H]-	0.498	17.6464	1.72E+04	713.42881	A2, A3, SW3
Amphidinolide K	[M-H]-	0.934	9.6758	3.60E+04	443.28045	SW3, SW4
Amphidinolide K	[M-H]-	0.947	10.1724	8.40E+04	443.28018	SW3, SW4
Amphidinolide K	[2M-H]-	0.746	14.9806	4.06E+04	887.569	A2, A3, SW3
Amphidinolide M	[M-H]-	0.233	14.0027	4.37E+04	725.46063	B01, BE1, AR1, AR2, A2, A3, SW3, SW4
Amphidinolide N	[M-H]-	0.959	4.0443	1.88E+04	641.35438	SW3, SW4
Amphidinolide N	[M-H]-	0.931	4.5737	2.57E+04	641.35447	SW3, SW4
Amphidinolide N	[M-H]-	0.871	4.909	1.04E+04	641.35466	SW3
Amphidinolide P	[M-H]-	0.955	9.4191	5.62E+03	373.20196	A2, A3
Amphidinolide P	[M-H]-	0.94	9.4876	1.35E+04	373.20194	A2, A3
Amphidinolide Q	[2M-	0.104	16.2703	6.95E+04	699.48101	A2, A3

	H]-					
Amphidinolide Q	[2M-H]-	0.936	18.2521	4.53E+04	699.48437	A2, A3
Amphidinolide Q	[2M-H]-	0.737	18.4656	1.68E+04	699.48506	A2, A3
Amphidinolide T1/T3-T5	[M-H]-	0.882	11.8941	6.03E+04	421.2957	A2
Amphidinolide X	[M-H]-	0.779	5.435	2.81E+04	447.27472	SW3, SW4
Amphidinolide X	[M-H]-	0.768	7.1376	1.26E+06	447.27469	SW3, SW4
Amphidinolide X	[M-H]-	0.756	7.924	1.22E+05	447.27467	SW3, SW4
Amphidinolide X	[M-H]-	0.739	8.0511	7.35E+05	447.27463	SW3, SW4
Amphidinolide X	[M-H]-	0.802	8.2563	3.29E+05	447.27477	SW3, SW4
Amphidinolide X	[M-H]-	0.82	9.0773	8.79E+04	447.27481	SW3, SW4
Amphidinolide X	[M-H]-	0.866	12.7476	1.14E+05	447.27551	A2, A3, SW3, SW4
Amphidinolide X	[M-H]-	0.877	12.9392	1.08E+05	447.27549	A2, A3, SW4
Amphidinolide Y	[M-H]-	0.826	9.3498	1.35E+04	449.29047	SW4
Dinophysistoxin 1	[M-H]-	0.959	10.9542	4.16E+04	817.47453	Standard
Dinophysistoxin 1	[M-H]-	0.916	11.6215	2.57E+06	817.47402	Standard
Iriometeolide 1a/1b	[M-H]-	0.852	5.435	6.53E+05	505.3167	SW3, SW4
Iriometeolide 1a/1b	[M-H]-	0.86	6.1708	6.47E+05	505.31672	SW3, SW4

Iriometeolide 1a/1b	[M-H]-	0.94	6.4368	2.26E+05	505.31693	SW3, SW4
Iriometeolide 1a/1b	[M-H]-	0.964	7.1293	3.94E+05	505.31699	SW3, SW4
Iriometeolide 1a/1b	[M-H]-	0.955	8.0686	1.95E+05	505.31696	SW3, SW4
Iriomoteolide 12a	[2M-H]-	0.259	11.9111	6.51E+04	839.56476	A2
Iriomoteolide 1c	[M-H]-	0.825	7.1376	1.40E+06	519.33227	SW3, SW4
Iriomoteolide 1c	[M-H]-	0.79	8.06	8.18E+05	519.33218	SW3, SW4
Iriomoteolide 1c	[M-H]-	0.831	8.2563	6.20E+05	519.33229	SW3, SW4
Iriomoteolide 1c	[M-H]-	0.982	8.5649	5.80E+05	519.33268	SW3, SW4
Iriomoteolide 1c	[M-H]-	0.929	10.0957	4.22E+04	519.33291	SW3, SW4
Iriomoteolide 1c	[M-H]-	0.587	10.5998	2.53E+05	519.33166	SW3, SW4
Iriomoteolide 1c	[2M-H]-	0.59	13.611	4.87E+04	1039.6706	SW3, SW4
Iriomoteolide 3a	[M-H]-	0.904	8.6194	2.05E+04	433.25936	SW3
Iriomoteolide 3a	[M-H]-	0.789	9.3357	4.08E+04	433.25911	SW3
Iriomoteolide 3a	[2M-H]-	0.923	17.3437	7.20E+04	867.52607	A2
Iriomoteolide 3a	[2M-H]-	0.959	17.5026	1.59E+06	867.52622	A2, A3, SW3, SW4